

ELECTROSPUN FISH SKIN GELATIN SCAFFOLDS FOR  
FUNCTIONAL TISSUE ENGINEERING OF ARTICULAR CARTILAGE

KHOO WEILY

A thesis submitted in  
fulfillment of the requirement for the award of the  
Doctor of Philosophy in Mechanical Engineering



PTTA UTHM  
PERPUSTAKAAN TUNKU TUN AMINAH

Faculty of Mechanical and Manufacturing Engineering  
Universiti Tun Hussein Onn Malaysia

NOVEMBER 2021

## ACKNOWLEDGEMENT

First and foremost, I would like to express my sincerest appreciation to my research supervisor, Dr. Koh Ching Theng, who provided me endless guidance and supports throughout the duration of this project. Furthermore, my gratitude also goes to my research co-supervisor, Dr. Sharaniza Ab. Rahim, who provided me professional training and assistance in cell culture basics. I am very thankful for all of her valuable comments and guidance during this project. Without their guidance and assistance, this research would not have been possible. Many thanks!

Moreover, I am particularly grateful for the assistance given by Mr. Anuar Ismail and Mr. Tarmizi Nasir from Faculty of Mechanical and Manufacturing Engineering as well as Mr. Zakaria Jazuli from Faculty of Engineering Technology. Besides, I wish to acknowledge the cooperation given and knowledge shared by coworkers and staffs in Institute of Medical Molecular Biotechnology (IMMB), Universiti Teknologi MARA, Sungai Buloh Campus. It was fantastic to have opportunity to conduct the research work in IMMB. My appreciation also goes to everyone involved directly or indirectly towards the compilation of this project.

I would like to take this opportunity to deliver my gratitude for the financial funding provided from Research Fund UTHM and Ministry of Education Malaysia. And finally, last but not least, my special gratitude also extends to my family members including my husband and my late father. Thanks for all the encouragement, guidance and supports given throughout this research.

## ABSTRACT

Articular cartilage is a soft tissue that covers bone joint surface. It has very low self-regenerative potential after injury, owing to its avascular nature. In recent years, hydrogels have been extensively studied as tissue engineering scaffolds for damaged articular cartilage. However, the use of fish skin gelatin as articular cartilage tissue engineering scaffold is remained unclear. Accordingly, the ultimate goal of this project is to investigate the feasibility of fish skin gelatin scaffold for articular cartilage tissue engineering application. Fish skin gelatin solution was first electrospun into fibrous scaffold under different solution feed rate (0.15 ml/h to 0.60 ml/h), applied voltage (9 kV to 18 kV) and spinning distance (10 cm to 25 cm). The scaffolds were visualized under SEM and mechanically tested in uniaxial tension and fracture mode I at displacement rate of 3 mm/min. Results revealed that scaffolds with fiber diameters ranged from  $199 \pm 15.75$  nm to  $795 \pm 89.91$  nm have been produced at different process parameters. After crosslinking with GA vapor, scaffolds were found to maintain their fibrous structure with improved aqueous stability and mechanical properties. The elastic modulus and fracture toughness of crosslinked scaffolds was found to achieve up to  $363.50 \pm 61.83$  MPa and  $8.81 \pm 1.91$  kJ/m<sup>2</sup> respectively. The crosslinked electrospun scaffolds were stiffer and tougher than that of articular cartilage. Moreover, *in vitro* culture of human chondrocytes on scaffold revealed that fish skin gelatin scaffolds supported cell proliferation and attachment as well as ECM production. Besides that, in an attempt to mimic the layered structure and function of articular cartilage, graded electrospun scaffold was produced using sequential electrospinning process. Such scaffold presented gradually change in fiber diameter and packing density over the thickness. Overall, electrospun fish skin gelatin scaffolds produced in present work showed great promise for articular cartilage tissue engineering since they were mechanically stiff yet tough scaffolds which supported cell proliferation and GAGs accumulation.

## ABSTRAK

Rawan artikular ialah tisu penghubung lembut yang meliputi permukaan sendi tulang. Selepas mengalami kecederaan, ianya kurang berupaya untuk pulih kerana sifat ketiadaan saluran darah. Dalam beberapa tahun kebelakangan ini, hidrogel telah banyak dikaji sebagai *scaffold* untuk kejuruteraan tisu rawan artikular. Namun, penggunaan gelatin dari kulit ikan sebagai *scaffold* untuk kejuruteraan tisu rawan artikular masih tidak jelas. Oleh itu, tujuan utama projek ini ialah mengkaji kebolehlaksanaan *scaffold* gelatin kulit ikan untuk aplikasi kejuruteraan tisu rawan artikular. Larutan gelatin dari kulit ikan telah digunakan untuk menghasilkan *scaffold* serat pada kadar suapan (0.15 ml/j hingga 0.60 ml/j), voltan (9 kV hingga 18 kV) dan jarak (10 cm hingga 25 cm) yang berbeza. *Scaffold* kemudiannya dilihat dalam mikroskop electron imbasan serta diuji dalam ujian tegangan dan ujian patah mod I pada kadar anjakan 3 mm/minit. Dalam projek ini, *scaffold* serat yang berdiameter  $199 \pm 15.75$  nm hingga  $795 \pm 89.91$  nm telah diperolehi pada proses parameter yang berbeza. Selepas paut silang dengan wap *glutaraldehyde* (GA), struktur serat *scaffold* masih kekal. Kestabilan *scaffold* dalam larutan akueus dan sifat mekanikalnya juga bertambah baik. Modulus elastik dan ketahanan patah *scaffold* masing-masing boleh mencapai  $363.50 \pm 61.83$  MPa dan  $8.81 \pm 1.91$  kJ/m<sup>2</sup>. Ianya lebih kaku and kuat daripada rawan artikular. Tambahan pula, *scaffold* tersebut juga dapat menggalakan percambahan sel, lampiran sel dan pengeluaran matriks ekstraselular dalam *vitro* apabila kondrosit manusia ditumbuhkan padanya. Selain itu, dalam usaha menyerupai struktur dan fungsi rawan artikular, *scaffold* yang mempunyai perubahan diameter dan ketumpatan serat sepanjang ketebalannya telah dihasilkan. Secara keseluruhan, *scaffold* yang dihasilkan dalam projek ini sesuai untuk kejuruteraan tisu rawan artikular kerana mereka mempunyai sifat mekanikal yang kaku dan kuat serta menyokong percambahan sel dan pengumpulan glikosaminoglikan.

## CONTENTS

<b>TITLE</b>	<b>i</b>
<b>DECLARATION</b>	<b>ii</b>
<b>ACKNOWLEDGEMENT</b>	<b>iii</b>
<b>ABSTRACT</b>	<b>iv</b>
<b>ABSTRAK</b>	<b>v</b>
<b>CONTENTS</b>	<b>vi</b>
<b>LIST OF TABLES</b>	<b>xiii</b>
<b>LIST OF FIGURES</b>	<b>xiv</b>
<b>LIST OF SYMBOLS AND ABBREVIATIONS</b>	<b>xxi</b>
<b>LIST OF APPENDICES</b>	<b>xxiii</b>
<b>CHAPTER 1 INTRODUCTION</b>	<b>1</b>
1.1 Research Background	1
1.2 Problem Statement	4
1.3 Objectives of Study	6
1.4 Scopes of Study	7
1.5 Significance of Study	8
1.6 Organization of Thesis	9
<b>CHAPTER 2 LITERATURE REVIEW</b>	<b>11</b>
2.1 Introduction to Articular Cartilage	11
2.1.1 Composition of articular cartilage	12
2.1.2 Hierarchical structure of articular cartilage	13
2.1.3 Structure and zonal organization of articular cartilage	15



PTTA UTHM

PERPUSTAKAAN TUNKU TUN AMINAH

2.2	Biomechanical Properties of Articular Cartilage	18
2.2.1	Tensile properties of articular cartilage	19
2.2.1.1	Zonal variations of articular cartilage in mechanical properties	22
2.2.2	Fracture of articular cartilage	23
2.3	Articular Cartilage Tissue Engineering	25
2.3.1	Scaffold requirements	26
2.3.2	Hydrogels as scaffold materials	27
2.3.2.1	Methods in enhancing hydrogels properties	28
2.4	Electrospinning as Fabrication Methods of Fibrous Scaffolds	31
2.4.1	Electrospinning process	32
2.4.2	Electrospun microstructure morphology control	34
2.4.2.1	Control of beads formation	34
2.4.2.2	Control of fiber diameter	38
2.5	Influences of Fiber Diameter on Scaffolds' Properties and Cell Responses	41
2.5.1	Scaffolds' physical and mechanical properties	42
2.5.2	Cell responses	44
2.6	Functional Graded Scaffold	47
2.7	Summary	49

### **CHAPTER 3 RESEARCH METHODOLOGY** **53**

3.1	Introduction	53
3.2	Materials	59
3.2.1	Fabrication of electrospun scaffolds	59
3.2.2	<i>In vitro</i> cell culture and testing	59
3.3	Electrospinning Machine Setup	60
3.4	Fabrication of Electrospun Fish Skin Gelatin Scaffolds	61

3.4.1	Solution preparation	61
3.4.2	Fabrication of homogenous scaffolds	62
3.4.2.1	Parametric studies on electrospinning process parameters	62
3.4.2.2	Smallest and largest fiber diameter of electrospun scaffolds	63
3.4.3	Fabrication of functional graded scaffolds	64
3.5	Crosslinking of Electrospun Scaffolds with Glutaraldehyde (GA) Vapor	65
3.5.1	Method I	65
3.5.2	Method II	66
3.5.3	Method III	66
3.6	Characterization of Electrospun Scaffolds	67
3.6.1	Fish skin gelatin solution viscosity measurement	67
3.6.2	Morphology and cross section observation and quantification	68
3.6.3	Topology observation	69
3.7	Mechanical Testing of Electrospun Scaffolds	69
3.7.1	Sample preparation	70
3.7.2	Uniaxial tensile test	71
3.7.3	Fracture test	72
3.7.3.1	Determination of fracture toughness	72
3.7.3.2	Observation on failure mechanism	73
3.8	Swelling Test	73
3.9	Degradation Test	74
3.10	<i>In Vitro</i> Cell Culture and Assay	74
3.10.1	Sample preparation and <i>in vitro</i> cell culture	74



3.10.2	Cell proliferation assay	75
3.10.3	Cell morphology observation	76
3.10.4	Biochemical assay	76
3.10.4.1	Protein extraction using Radio Immuno Precipitation Assay (RIPA) buffer	76
3.10.4.2	Bradford assay	77
3.10.4.3	Glycosaminoglycans (GAGs) assay	78
3.11	Statistical Analysis	79

## **CHAPTER 4 MICROSTRUCTURE MORPHOLOGY AND MECHANICAL PERFORMANCES OF ELECTROSPUN SCAFFOLDS 81**

4.1	Introduction	81
4.2	Solution Viscosity	82
4.3	Morphology of Electrospun Scaffolds	83
4.3.1	Fiber diameter of electrospun scaffolds	83
4.3.2	Smallest and largest fiber diameter of electrospun scaffold	87
4.3.3	Morphological characteristic of electrospun scaffolds	90
4.4	Mechanical Performances of Electrospun Scaffolds	93
4.4.1	Tensile properties	93
4.4.2	Fracture properties	96
4.4.3	Failure mechanism of electrospun scaffolds	99
4.5	Discussion	100
4.5.1	Solution viscosity over storage time	100
4.5.2	Parametric studies on electrospinning process parameters	101
4.5.3	Smallest and largest fiber diameter of electrospun scaffold	103



4.5.4	Morphological characteristics of electrospun scaffolds	105
4.5.5	Mechanical properties of electrospun scaffolds	107
4.6	Summary	109

**CHAPTER 5 EFFECTS OF CROSSLINKING METHODS ON ELECTROSPUN SCAFFOLD'S PERFORMANCES**

		<b>110</b>
5.1	Introduction	110
5.2	Visual Appearance of Electrospun Scaffolds	111
5.3	Morphology of Electrospun Scaffolds	112
5.4	Topology of Electrospun Scaffolds	114
5.5	Mechanical Performances of Electrospun Scaffolds	116
5.6	Swelling and Degradation Properties	118
5.6.1	Swelling properties	119
5.6.2	Degradation properties	119
5.7	Discussion	120
5.7.1	Appearance, morphology and topology of crosslinked scaffolds	121
5.7.2	Mechanical performances of crosslinked scaffolds	122
5.7.3	Swelling and degradation properties of crosslinked scaffolds	123
5.7.4	Methods in enhancing hydrogels' mechanical properties	125
5.8	Summary	127

**CHAPTER 6 *IN VITRO* CELL RESPONSES AND PERFORMANCES OF CROSSLINKED ELECTROSPUN SCAFFOLDS**

6.1	Introduction	129
6.2	Morphology of Electrospun Scaffolds	130

6.3	Mechanical Performances of Electrospun Scaffolds	132
6.4	Swelling and Degradation Properties	134
6.4.1	Swelling properties	134
6.4.2	Degradation properties	135
6.5	<i>In Vitro</i> Test Result	135
6.5.1	Cell proliferation	135
6.5.2	Cell morphology	137
6.5.3	Biochemical evaluation	139
6.6	Discussion	140
6.6.1	Influence of fiber diameter on chondrocytes responses <i>in vitro</i>	140
6.6.2	Influence of fiber diameter on cartilage formation <i>in vitro</i>	143
6.6.3	Mechanical performance comparison with native soft tissues	145
6.7	Summary	147
<b>CHAPTER 7 FUNCTIONAL GRADED ELECTROSPUN SCAFFOLD FOR ARTICULAR CARTILAGE TISSUE ENGINEERING APPLICATION</b>		<b>148</b>
7.1	Introduction	148
7.2	Morphology and Cross Section of Graded Electrospun Scaffold	149
7.3	Mechanical Performances of Graded Electrospun Scaffold	150
7.4	Swelling and Degradation Properties	154
7.5	Discussion	155
7.5.1	Fabrication method of functional graded scaffold	155
7.5.2	Mechanical performances of functional graded scaffold	157
7.5.3	Mechanical performances comparison with native soft tissues	158



	xii
7.6 Summary	160
<b>CHAPTER 8 CONCLUSION AND RECOMMENDATIONS</b>	<b>161</b>
8.1 Conclusion	161
8.2 Recommendations	164
<b>REFERENCES</b>	<b>166</b>
<b>APPENDIX</b>	<b>197</b>
<b>VITA</b>	<b>199</b>



## LIST OF TABLES

Table 2.1: Summary of component morphology, size and composition of four distinct articular cartilage regions	18
Table 2.2: Zonal variations in mechanical properties of human articular cartilage	22
Table 2.3: The beads formation on electrospun scaffolds under different electrospinning parameters	36
Table 2.4: The fiber diameter of electrospun scaffolds under different electrospinning parameters	39
Table 3.1: List of materials used for electrospun scaffolds fabrication	59
Table 3.2: List of materials used for <i>in vitro</i> cell culture and assay	60
Table 3.3: The experimental setting in the electrospinning process. The process parameters studies were categorized into three groups: tip-collector distance (group A), solution feed rate (group B), and applied voltage (group C)	63
Table 3.4: The experimental setting in obtaining smallest (group A) and largest (group B and C) fiber diameter of electrospun scaffold	64
Table 3.5: The experimental setting for functional graded scaffolds fabrication	65
Table 3.6: Crosslinking methods for electrospun fish gelatin scaffolds	65
Table 3.7: Diluted BSA Standards preparation	77
Table 3.8: GAG standards solution preparation	78



PTAAUTHM

PERPUSTAKAAN TUN KU TUN AMINAH

## LIST OF FIGURES

Figure 1.1: Appearance of healthy and damaged articular cartilage in knee (Harris & Flanigan, 2011)	1
Figure 1.2: Composition and morphology of healthy, early stage osteoarthritic and advanced osteoarthritic articular cartilage (Oei <i>et al.</i> , 2014)	2
Figure 1.3: Treatments approaches for damaged articular cartilage (Kwon <i>et al.</i> , 2019)	3
Figure 2.1: Schematic illustration of hierarchical structure of the articular cartilage over different length scale (adapted from Mow <i>et al.</i> , 1992)	14
Figure 2.2: Zonal organization of collagen fibrils in an articular cartilage (adapted from Mow <i>et al.</i> , 1992)	15
Figure 2.3: Zonal organization of chondrocytes in an articular cartilage (adapted from Mow <i>et al.</i> , 1992)	16
Figure 2.4: Stress-strain curve of an articular cartilage, showing nonlinear tensile behavior (Cohen <i>et al.</i> , 1998)	21
Figure 2.5: Five stages of crack growth in articular cartilage (Stok & Oloyede, 2003)	24
Figure 2.6: Tissue engineering approaches	26
Figure 2.7: Basic setup of electrospinning apparatus in vertical configuration	33
Figure 2.8: The Taylor cone formation and spinning jet initiation when high voltage is supplied	34
Figure 2.9: Beads formation on electrospun gelatin scaffold (Kwak <i>et al.</i> , 2017)	35

Figure 2.10: SEM photographs of electrospun gelatin scaffolds produced at solution concentration of (a) 7.5 w/v % and (b) 12.5 w/v % (Huang <i>et al.</i> , 2004)	39
Figure 2.11: Pore area of electrospun PCL/collagen scaffold with four different fiber diameters (Ju <i>et al.</i> , 2010)	42
Figure 2.12: Morphology of chondrocytes seeded on PLLA microfibrinous and nanofibrinous scaffold (Li <i>et al.</i> , 2006)	46
Figure 2.13: Scaffold with graded microstructure which produced by using (a) additive manufacturing (Di Luca, Szlazak, <i>et al.</i> , 2016), (b) electrospinning (Grey <i>et al.</i> , 2013), (c) centrifugation method (Oh <i>et al.</i> , 2007) and (d) layer by layer assembly (Wu <i>et al.</i> , 2008)	48
Figure 3.1: Flow chart for Section A	55
Figure 3.2: Flow chart for Section B	56
Figure 3.3: Flow chart for Section C	57
Figure 3.4: Flow chart for Section D	58
Figure 3.5: Electrospinning machine used in this study	61
Figure 3.6: Crosslinking of electrospun fish gelatin scaffold in Method I	66
Figure 3.7: Fish skin gelatin scaffold clipped with binder clips	67
Figure 3.8: Lloyd Instruments Ltd LR30K type UTM	70
Figure 3.9: Schematic illustration of sample geometries for (a) uniaxial tensile test and (b) fracture test	71
Figure 4.1: Fish skin gelatin solution viscosity over storage time	82
Figure 4.2: SEM images of electrospun fish gelatin scaffolds obtained at applied voltage of 15 kV, solution feed rate of 0.30 ml/h and tip-collector distance of (a) 10 cm, (b) 15 cm, (c) 20 cm and (d) 25 cm. All scale bars represent 5 $\mu$ m in length	83
Figure 4.3: SEM images of fish gelatin electrospun scaffolds obtained at applied voltage of 15 kV and tip-collector distance of 20 cm and solution feed rate of (a) 0.15 ml/h, (b) 0.30 ml/h, (c) 0.45 ml/h and (d) 0.60 ml/h. All scale bars represent 5 $\mu$ m in length	84
Figure 4.4: SEM images of fish gelatin electrospun scaffolds obtained at tip-collector distance of 20 cm and solution feed rate of 0.30	

ml/h and applied voltage of (a) 9 kV, (b) 12 kV, (c) 15 kV and (d) 18 kV. All scale bars represent  $5 \mu\text{m}$  in length 85

Figure 4.5: Fiber diameters of electrospun fish skin gelatin scaffolds as a function of (a) tip-collector distance,  $d$ , (b) solution feed rate,  $f$  and (c) applied voltage,  $v$  86

Figure 4.6: SEM images of electrospun scaffold produced at applied voltage of 9 kV, tip-collector distance of 20 cm and solution feed rate of (a) 0.15 ml/h, (b) 0.30 ml/h, (c) 0.45 ml/h and (d) 0.60 ml/h. All scale bars represent  $5 \mu\text{m}$  in length 87

Figure 4.7: SEM images of electrospun scaffold produced at applied voltage of 15 kV, tip-collector distance of 15 cm and solution feed rate of (a) 0.15 ml/h, (b) 0.30 ml/h, (c) 0.45 ml/h and (d) 0.60 ml/h. All scale bars represent  $5 \mu\text{m}$  in length 88

Figure 4.8: SEM images of electrospun scaffold produced at applied voltage of 18 kV, tip-collector distance of 15 cm and solution feed rate of (a) 0.15 ml/h, (b) 0.30 ml/h, (c) 0.45 ml/h and (d) 0.60 ml/h. All scale bars represent  $5 \mu\text{m}$  in length 89

Figure 4.9: Fiber diameters of electrospun fish skin gelatin scaffolds produced at (a) applied voltage,  $v$  of 9 kV and tip-collector distance,  $d$  of 20 cm and at (b) applied voltage,  $v$  of 15 kV and 18 kV and tip-collector distance,  $d$  of 15 cm 90

Figure 4.10: The effects on (a) pore size and (b) total pore area as the function of fiber diameter 91

Figure 4.11: The effects on (a) fiber area, (b) fiber length, (c) fiber density, (d) fiber volume, (e) volume ratio and (f) porosity as the function of fiber diameter 92

Figure 4.12: Stress strain curves of electrospun fish skin gelatin scaffolds consisted of different mean fiber diameters, ranging from 199 nm to 795 nm 93

Figure 4.13: Elastic properties of electrospun fish skin gelatin scaffold in term of (a) tensile strength and (b) elastic modulus as a function of fiber diameter 95

- Figure 4.14: Stress strain curves of fracture test samples for electrospun fish skin gelatin scaffolds consisted of different mean fiber diameters, ranging from 199 nm to 795 nm 96
- Figure 4.15: Fracture properties of electrospun fish skin gelatin scaffold in term of (a) fracture strain and (b) fracture toughness as a function of fiber diameter 99
- Figure 4.16: Failure mechanism of electrospun fish skin gelatin scaffolds in the vicinity of notch tip, as visualized under SEM. The SEM images are presented for electrospun scaffold with mean fiber diameter of (a – c) 795 nm and (d – f) 199 nm. Scaffold was deformed by strain (a)  $\varepsilon_0 = 0.12$ , (b)  $\varepsilon_1 = 0.14$  and (c)  $\varepsilon_2 = 0.19$ . Scaffold was deformed by strain (d)  $\varepsilon_0 = 0.22$ , (e)  $\varepsilon_1 = 0.25$  and (f)  $\varepsilon_2 = 0.85$  100
- Figure 4.17: Comparison of fiber diameter collected at tip-collector distance of 15 cm and 20 cm, applied voltage of 15 kV and 18 kV and solution feed rate of 0.30 ml/h 105
- Figure 4.18: Influences of volume ratio on (a) tensile strength,  $\sigma_f$ , (b) elastic modulus,  $E$ , (c) fracture strain,  $\varepsilon_f$ , and (d) fracture toughness,  $G_c$  of electrospun fish skin gelatin scaffolds 108
- Figure 5.1: Fish skin gelatin scaffold before and after crosslinking process. (a) UFG scaffold, (b) WOF\_25 scaffold, (c) WOF\_5 scaffold and (d) WF\_5 scaffold. All scale bars represent 5 cm in length 111
- Figure 5.2: Morphology of (a) UFG scaffold, (b) WOF\_25 scaffold, (c) WOF\_5 scaffold and (d) WF\_5 scaffold. All scale bars represent 5  $\mu\text{m}$  in length 112
- Figure 5.3: Quantification of (a) fiber diameters and (b) pore sizes for electrospun fish skin gelatin scaffolds before and after crosslinking at different methods 113
- Figure 5.4: 3D topology images of (a, c and e) top surface and (b, d and f) bottom surface of WOF\_25 scaffold, WOF\_5 scaffold and WF\_5 scaffold 115



Figure 5.5: Stress strain responses of WOF_25 scaffold, WOF_5 scaffold and WF_5 scaffold under (a, c and e) uniaxial tensile test and (b, d and f) fracture test	116
Figure 5.6: Mechanical performances of fish skin gelatin scaffolds before and after crosslinking process. (a) Tensile strength $\sigma_f$ , (b) elastic modulus $E$ , (c) fracture strain $\epsilon_f$ , and (d) fracture toughness $G_c$	118
Figure 5.7: Swelling percentage of crosslinked scaffolds	119
Figure 5.8: Degradation percentage of crosslinked scaffolds	120
Figure 5.9: Fracture toughness versus elastic modulus for fish skin gelatin scaffolds compared to other hydrogels (Naficy <i>et al.</i> , 2011; Sun <i>et al.</i> , 2012; Tonsomboon <i>et al.</i> , 2017) and mechanical enhancement strategies from previous studies (Naficy <i>et al.</i> , 2011; Sun <i>et al.</i> , 2012; Li, Illeperuma, <i>et al.</i> , 2014; Li, Suo & Vlassak, 2014; Tonsomboon <i>et al.</i> , 2017)	125
Figure 6.1: Comparison of the microstructure of two types of electrospun scaffold. The SEM images of SFD electrospun scaffold taken (a) before and (b) after crosslinking and LFD electrospun scaffold taken (c) before and (d) after crosslinking. All scale bars represent $5 \mu\text{m}$ in length	130
Figure 6.2: Changes of scaffold network architecture after crosslinking. SFD scaffold consists of fiber diameter of (a) 199 nm changing to 875 nm after crosslinking. Meanwhile, LFD scaffold consists of fiber size of (b) 795 nm changing to 1534 nm after crosslinking	131
Figure 6.3: Stress-strain curves of SFD and LFD scaffolds before and after the crosslinking process	132
Figure 6.4: Mechanical performances of SFD and LFD scaffolds measured before and after crosslinking	133
Figure 6.5: Swelling percentage of fish skin gelatin scaffolds after 24 hours of immersion in PBS solution	134
Figure 6.6: Degradation percentage of SFD and LFD scaffolds up to 8 days of immersion in PBS solution	135

- Figure 6.7: Proliferation of chondrocytes cultured on crosslinked SFD and LFD scaffolds as a function of time. Cell proliferation of both types of scaffolds was normalized with control sample. An asterisk (\*) indicates statistical difference ( $p < 0.05$ ) in between scaffolds 136
- Figure 6.8: Morphology of chondrocytes seeded on SFD scaffold (a, c and e) and LFD scaffold (b, d and f) after 8 days of culture. Arrow heads in (e and f) indicate cell adhesion and interaction on scaffolds 138
- Figure 6.9: Results of biochemical assays on chondrocytes seeded SFD and LFD scaffold over 8 days of culture period. An asterisk (\*) indicates statistical difference ( $p < 0.05$ ) in between scaffolds 139
- Figure 6.10: Chondrocytes' attachment, spreading and morphology on (a) SFD and (b) LFD scaffolds. (a) Serum from the cell culture medium was attached to the fibers, making a bed for chondrocytes to attach and spread more on SFD scaffold. (b) Filopodia tips from edges of chondrocytes were spiked on LFD scaffold, showing less attachment on the scaffold. The spherical shape of chondrocytes was preserved on LFD scaffold 142
- Figure 6.11: Fracture toughness  $G$  versus elastic modulus  $E$  for fish skin gelatin scaffolds compared to hydrogels, native soft tissues, and mechanical enhancement strategies reported from previous studies 146
- Figure 7.1: Architecture of graded electrospun fish skin gelatin scaffold. (a) SEM image for cross section of graded scaffold. Scale bar is 500  $\mu\text{m}$ . (b) High magnification of SEM images for cross section of the graded scaffold, enclosed by rectangular boxes in (a). Scale bars are 50  $\mu\text{m}$ . (c) SEM images for morphology of each layer in the graded scaffold. Scale bar indicate 5  $\mu\text{m}$  149

- Figure 7.2: Stress strain responses of graded electrospun fish skin gelatin scaffold under uniaxial tensile test and fracture test 150
- Figure 7.3: Failure mechanism of graded electrospun fish skin gelatin scaffold visualized under SEM. The scaffold was deformed by strain (a and e)  $\varepsilon_0 = 0.05$ , (b and f)  $\varepsilon_1 = 0.11$ , (c and g)  $\varepsilon_2 = 0.29$  and (d and h)  $\varepsilon_3 = 0.33$  152
- Figure 7.4: Stress strain responses of crosslinked graded electrospun fish skin gelatin scaffold under uniaxial tension and fracture test 153
- Figure 7.5: Mechanical performances of graded electrospun fish skin gelatin scaffolds measured before and after crosslinking 154
- Figure 7.6: Swelling and degradation percentage of graded electrospun fish skin gelatin scaffold before and after crosslinking process 155
- Figure 7.7: Fracture toughness  $G$  versus elastic modulus  $E$  for graded fish skin gelatin scaffold compared with homogenous fish skin gelatin scaffolds and native soft tissues 159



## LIST OF SYMBOLS AND ABBREVIATIONS

AFM	Atomic Force Microscope
BMSCs	Bone Marrow Mesenchymal Stem Cells
BSA	Bovine Serum Albumin
BSE	Bovine Spongiform Encephalopathy
<i>d</i>	Tip to Collector Distance
DMEM	Dulbecco's Modified Eagle's Medium
DMF	Dimethylformamide
DN	Double Network
ECM	Extracellular Matrix
<i>E</i>	Elastic Modulus
<i>f</i>	Solution Feed Rate
FBS	Fetal Bovine Serum
GA	Glutaraldehyde
GAGs	Glycosaminoglycans
$G_c$	Fracture Toughness
LFD	Large Fiber Diameter
MSCs	Mesenchymal Stem Cells
MSEN	Modified Single Edge Notched Test
NSCs	Neural Stem/Progenitor Cells
PAN	Polyacrylonitrile
PBS	Phosphate Buffered Saline
PCL	Polycaprolactone
Pen Strep	Penicillin Streptomycin
PEO	Poly (ethylene oxide)
PLCL	Poly (L-lactide-co- $\epsilon$ -caprolactone)
PLGA	Poly (lactic-co-glycolic acid)

PLLA	Poly (L-lactide acid)
PS	Polystyrene
PVA	Poly (vinyl alcohol)
PVP	Poly (vinylpyrrolidone)
RIPA	Radio Immuno Precipitation Assay
SEM	Scanning Electron Microscopy
SFD	Small Fiber Diameter
TFE	2,2,2-Trifluoroethanol
UFG	Uncrosslinked Fish Skin Gelatin
UTM	Universal Testing Machine
$v$	Applied Voltage
$\sigma$	Stress
$\sigma_f$	Tensile Strength
$\varepsilon$	Strain
$\varepsilon_f$	Fracture Strain



PTTA UTHM  
PERPUSTAKAAN TUNKU TUN AMINAH

**LIST OF APPENDICES**

<b>APPENDIX</b>	<b>TITLE</b>	<b>PAGE</b>
A	Microarchitecture quantification and porosity calculation	197



## CHAPTER 1

### INTRODUCTION

#### 1.1 Research Background

Articular (hyaline) cartilage is a soft and flexible connective tissue covering the bone joint surface. It has thin, dense and glassy appearance and is mainly found on the articular surface of bones. Figure 1.1 illustrates the appearance of healthy and damaged articular cartilage in knee.

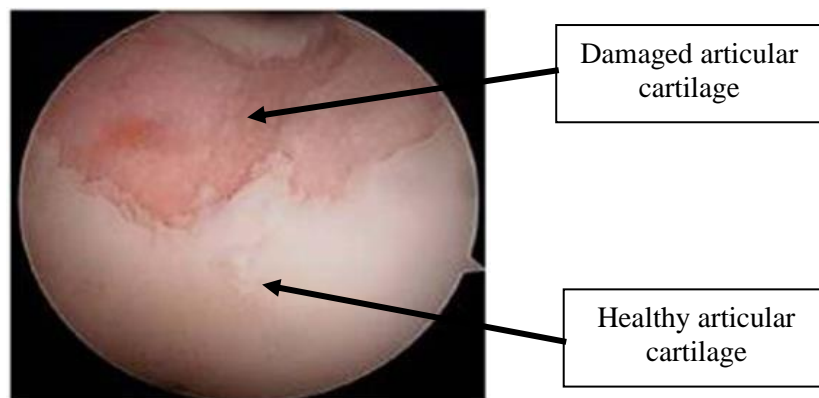


Figure 1.1: Appearance of healthy and damaged articular cartilage in knee (Harris & Flanigan, 2011)

Sport related injuries, degeneration due to disease, obesity and other types of damage can cause injuries to articular cartilage. Although chondrocytes tend to proliferate and synthesize extracellular matrix (ECM), their repair effectiveness to injury is limited. Moreover, chondrocytes typically suspend the reparative process before cartilage defect is healed (Zhang, Hu & Athanasiou, 2009). Continual degeneration will lead to osteoarthritis. Figure 1.2 demonstrates schematic illustrations of healthy, early stage osteoarthritic and advanced osteoarthritic articular cartilage. Changes in the tissue structure and cellular arrangement as well as the ECM components occurred when osteoarthritis progressed (Lorenz & Richter, 2006; Karim, Amin & Hall, 2018). Besides that, decline in mechanical properties was also noticed in osteoarthritis articular cartilage (Cooke *et al.*, 2018; Peter *et al.*, 2018). General activities and functions of joint will be limited. The injured joint will become swollen and patients will suffer from pain during movement. Without treatments in time or if the conservative (non-operative) therapies fail, the articular cartilage will wear away over time and may require knee surgery (Rönn *et al.*, 2011; Portocarrero, Collins & Livingston Arinzeh, 2013). Wilder *et al.* (2002) has reported that individuals who have history of knee injury were 7.4 times more likely to develop osteoarthritis than individuals who have not history of knee injury.

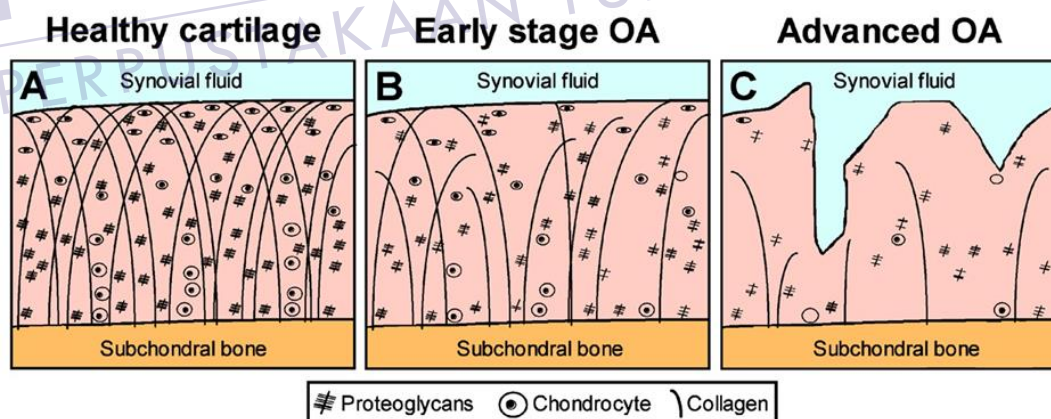


Figure 1.2: Composition and morphology of healthy, early stage osteoarthritic and advanced osteoarthritic articular cartilage (Oei *et al.*, 2014)

Owing to its avascular nature in which it possesses no nerves or blood vessels, articular cartilage has very low self-repair/regenerative potential after injury or degenerative disease. The limited self-repair/self-healing capacity of damaged



cartilage tissue has become interest among scientists and researchers to develop approaches in engineer articular cartilage. Figure 1.3 illustrates examples of treatment approaches for damaged articular cartilage. Most common current treatments for articular cartilage lesions rely on surgery procedures, which may include arthroscopic debridement, microfracture, osteochondral autograft transfer, autologous chondrocyte implantation, and partial or total knee arthroplasty (Rönn *et al.*, 2011; Portocarrero *et al.*, 2013; Rambani & Venkatesh, 2014; Kwon *et al.*, 2019; Roseti *et al.*, 2019).

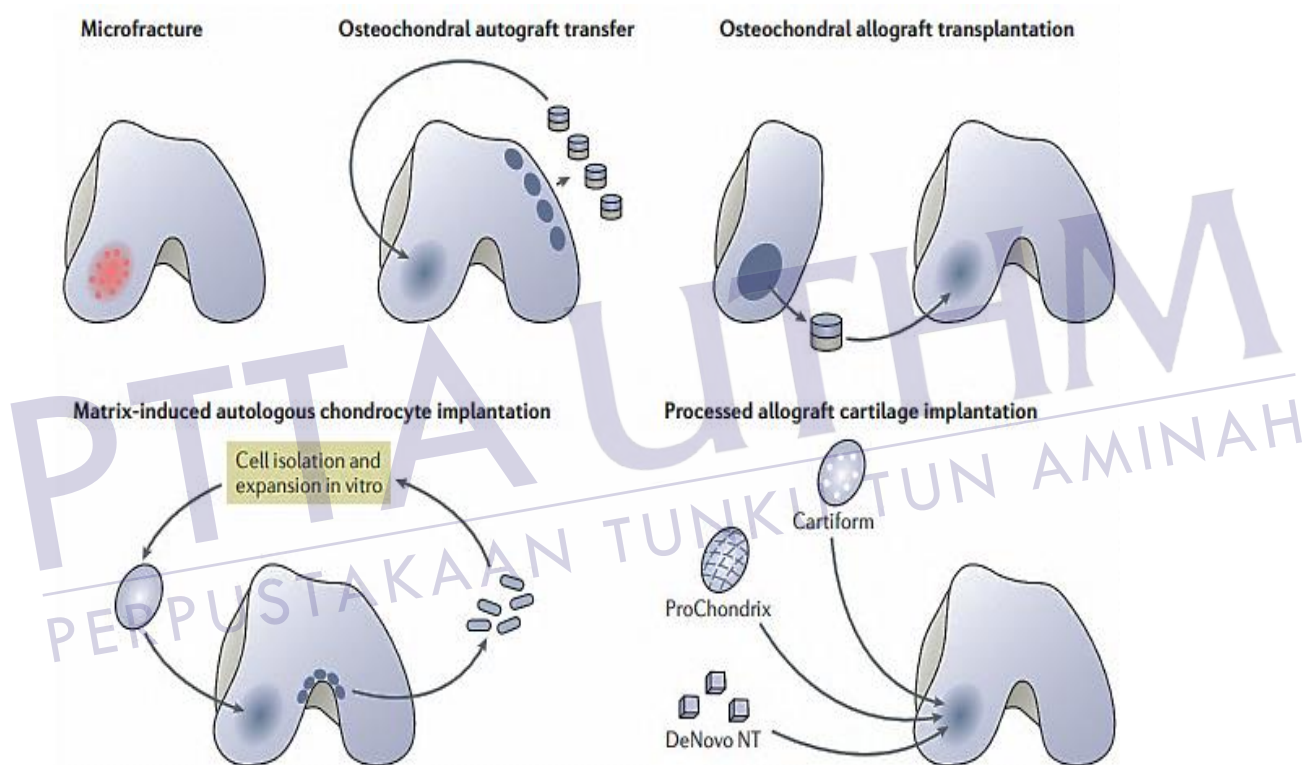


Figure 1.3: Treatments approaches for damaged articular cartilage (Kwon *et al.*, 2019)

Although scientists and surgeons have tried to improve current treatments and several strategies have been introduced in cartilage repair or regenerate over the years, there has been little success and no universally accepted successful treatment for articular cartilage injury. Overall, the outcomes of current treatments are still unsatisfying. For example, instead of repairing the damaged cartilage, arthroscopic technique removes the debris and inflammatory cytokines by shaving or smoothing the degenerated cartilage and this method is only a temporary treatment to reduce

symptoms (Rönn *et al.*, 2011; Portocarrero *et al.*, 2013). Besides, current treatments have their own limitations. In the case of autografts and allografts, the availability of grafts tissue in human body has limited its use in articular cartilage repair. Furthermore, two times operations are required for autologous chondrocyte implantation – harvest healthy chondrocyte in one operation and implant into the defected site in second operation after expansion in culture. For microfracture approaches, fibrocartilage typically forms, which is mechanically much less robust than articular cartilage (Portocarrero *et al.*, 2013). For severe osteoarthritis, joint arthroplasty is the only remedy but it is not suitable for patients younger than 60-years old and the prosthetic components will lose its durability after 15 – 20 years (Rönn *et al.*, 2011).

In recent years, articular cartilage tissue engineering has been found as an alternative approach for articular cartilage repair and regeneration. It is a intersect of scientific and technological field that focuses on development and application of knowledge in chemistry, physics, engineering, life and clinical sciences in order to solve the critical medical problems (Langer & Vacanti, 1993). In articular cartilage tissue engineering, many approaches have been done which focused on the development of artificial replacement (scaffold) that is functional resembling to the native extracellular matrix (ECM) of articular cartilage. A small amount of relevant healthy cells taken from human are cultured *in vitro* and seeded onto the scaffolds before transplantation onto human body. Such scaffolds are responsible to regenerate, maintain and improve the damaged tissue. Thus, it is believed that this strategy could be promising treatment method for patients with articular cartilage injuries.

## 1.2 Problem Statement

One of the key parameters that promise the outcome of tissue engineering is scaffold design (material and structure). To date, a wide range of scaffold materials have been extensively investigated for cartilage repair and regeneration. Hydrogels, a class of highly hydrated polymer materials, are promising scaffold materials for cartilage tissue engineering application, owing to their biocompatibility, cell affinity and biodegradable feature (Wei *et al.*, 2021). Among hydrogels, gelatin is one of the

most studied scaffold materials. It can be classified as mammalian gelatin or fish gelatin, according to its source. Although fish gelatin has been widely employed in different fields such as food industry, its use in articular cartilage tissue engineering applications remained unclear. Therefore, this study intended to use fish gelatin as the base material in preparing scaffold. Since fish gelatin presents highly hydrated and swelling feature which in turn influenced the mechanical properties of fish gelatin (Michelini *et al.*, 2020), method in improving water resistance and mechanical properties of fish gelatin was also investigated in this project.

Besides scaffold material, the structure of scaffolds also plays crucial role in ensuring the positive outcome of tissue engineering. Fibrous scaffolds have been extensively studied, due to their promise in mimicking the structure of tissues and also providing more favorable microenvironment for *in vitro* cells responses (Woo, Chen & Ma, 2003; Woo *et al.*, 2007). Previous finite element studies revealed that the mechanical properties of fibrous scaffolds were depended on many factors including their microstructural architecture, *e.g.*, fiber density (Koh & Oyen, 2015; Koh, Low & Yusof, 2015) and crosslinking density. However, there was still a lack of understanding in experimental work on the relationship between the microstructural architecture, in particular fiber diameter, and deformation and fracture of fibrous networks. Such understanding is critical in facilitating the production of fibrous scaffolds with predicted as well as improved mechanical properties.

In order to study the relationship between microstructural architecture and mechanical properties of fibrous scaffolds, it is therefore important to understand how their microstructural architecture can be altered. Fibrous scaffolds produced by electrospinning technique have been extensively studied as an ECM replacement for articular cartilage (Steele *et al.*, 2014). The microstructural architecture of fibrous scaffolds is governed by three main parameters, which are solution properties, process parameters and environmental factors (Sill & von Recum, 2008; Bhardwaj & Kundu, 2010; Repanas, Andriopoulou & Glasmacher, 2016). Existing studies have shown that changes in any electrospinning parameters can affect the morphology of resultant electrospun scaffold including beads formation and fiber diameter. Consequently, the mechanical behavior of fibrous scaffold will be affected due to the microstructure morphology variation. However, detailed understanding on how the electrospinning parameters affect electrospun fish skin gelatin scaffold morphology in micro length scale is still insufficient.

Native articular cartilage possesses zonal organization which distinguished by differences of cell morphologies and arrangement, collagen fibers orientation and mechanical properties. However, scaffold with homogenous materials composition or structural organization for single tissue regeneration is used typically in cartilage repair strategies. This shortcoming has consequently caused the resultant scaffolds become insufficient to mimic the complex composite tissue, which commonly exhibits gradient structural, compositional and functional properties. Hence, the development of scaffolds which mimic the gradient structure and properties of native articular cartilage is the current strategy employed in tissue engineering.

In current study, fish gelatin was electrospun into fibrous scaffold at different electrospinning process parameters including applied voltage, distance between needle tip and collector and also feed rate. The microstructure morphology and mechanical performance of these electrospun scaffolds were then assessed. The relationship between fiber diameter and tensile properties as well as fracture properties was determined. The electrospun scaffolds were further subjected to three different crosslinking processes to restrict the swelling characteristic and improve the mechanical properties of scaffold. *In vitro* test was then conducted on selected electrospun scaffolds to investigate the chondrocytes responses when seeded on different morphology. At the end of the project, structural and functional graded scaffold was developed with intention to mimic the fibrous microstructure and mechanical properties of articular cartilage.

### 1.3 Objectives of Study

This research is conducted specifically to achieve the following objectives:

1. To study on the mechanical performances of electrospun fish skin gelatin scaffolds by control their microstructure morphology at different electrospinning process parameters.
2. To investigate the effects of crosslinking methods on physical properties and mechanical properties of electrospun fish skin gelatin scaffolds.
3. To evaluate the influences of fiber diameter on mechanical properties and *in vitro* cell responses of the crosslinked electrospun fish skin gelatin scaffolds.

4. To develop and evaluate the functional graded electrospun fish skin gelatin scaffold for articular cartilage tissue engineering application.

#### 1.4 Scopes of Study

In order to achieve the objectives, the following scopes have been drawn.

1. This project covered fabrication of electrospun scaffolds using electrospinning technique. All the scaffolds were produced using customized electrospinning unit with horizontal configuration.
2. Fish skin gelatin was the only base material which used in preparing polymer solution for electrospinning process. The concentration of gelatin solution was maintained at 25 wt. % throughout the study.
3. In preparing electrospun scaffolds, only three electrospinning process parameters which were distance between needle tip and collector (10 cm to 25 cm), solution feed rate (0.15 ml/h to 0.60 ml/h) and also applied voltage (9 kV to 18 kV) were varied throughout present work.
4. The relative humidity of electrospinning chamber was kept constant at  $50 \pm 10$  % throughout the electrospinning process by using silica gels.
5. For the crosslinking agent for electrospun scaffolds, glutaraldehyde (GA) solution was used to create GA vapor during crosslinking process. The concentration of GA solution was only 5 % and 25 %.
6. The morphology and cross section of electrospun scaffolds were characterized using scanning electron microscopy (SEM). An image analysis software ImageJ was used to measure the diameter of electrospun fiber and to obtain the pore size of electrospun scaffolds.
7. The surface topology of crosslinked electrospun scaffold was visualized using atomic force microscope (AFM). Both top and bottom surfaces of each crosslinked scaffold were visualized.
8. The swelling and degradation behavior of electrospun scaffolds were monitored as the change in scaffold weight over time.
9. The mechanical performances of electrospun scaffolds covered uniaxial tensile test and fracture test. For uniaxial tensile test, it was conducted to

determine the stress-strain behavior, elastic modulus and also tensile strength of the electrospun scaffold. For fracture test, loading Mode I was used. The failure mechanism, failure strain as well as fracture toughness of electrospun scaffolds were determined under the fracture test.

10. Human chondrocyte was the only cell type which utilized in the *in vitro* study.

### 1.5 Significance of Study

While other studies focused on the reduction of morphological defects at different polymer solution properties, the significance of this study lies in the investigation of electrospinning process parameters including solution feed rate, applied voltage and also distance between needle tip and collector on fibrous fish skin gelatin scaffold's microstructural morphologies. Besides, the mechanical performances of fibrous scaffold including tensile and fracture properties were also studied to understand how the variation in fiber diameter affected the electrospun scaffold's mechanical properties. Such understanding can provide an insight for researchers in producing fish skin gelatin electrospun scaffold with desired fiber diameter and tailored mechanical properties.

Moreover, findings from this study also demonstrated that the electrospun fish skin gelatin scaffold was biocompatible to the human chondrocytes. The cells were able to attach, proliferate and remain viable during *in vitro* investigations period. Besides, results from present work also revealed the different chondrocytes responses and ECM production when they seeded on scaffold with different morphologies. These findings provide a new insight into cell-scaffold structure interactions which are important for understanding the responsibility of scaffold structure in leading cell responses and tissue formation.

Furthermore, the significance of this study also lies in the development of functional graded electrospun fish skin gelatin scaffold for articular cartilage tissue engineering application. By varying the process parameters in sequential electrospinning technique, scaffold with gradually changes in microstructure has been successfully produced. Such scaffold has successfully mimicked the fibrous microstructure and mechanical properties of native articular cartilage. Hence, the

scaffold has the potential to undergo *in vitro* and *in vivo* tests to further verify its feasibility in articular cartilage tissue engineering application.

## 1.6 Organization of Thesis

This PhD thesis is organized in eight chapters. Chapter 1 is the introduction on the research work. Chapter 2 is literature review on previous researches while Chapter 3 is the research methodology which used in this research work. Chapter 4 to Chapter 7 present the result and discussion on research findings. Chapter 8 is the conclusion and recommendations for future work.

Chapter 1 presents the background of this research work which briefly describes about the composition and morphology of healthy and damaged articular cartilage. The shortcomings of current treatments for damaged articular cartilage have also been discussed. The objectives, scope as well as significance of the research have also been presented in this chapter.

Chapter 2 reviews the findings and works published by previous researchers. Attention was first given on the structure and biomechanical properties of articular cartilage. Afterwards, electrospinning technique as fabrication method of fibrous scaffolds were studied as an alternative approach to replicate fibrous structure of articular cartilage. The influence of fiber diameter on scaffolds' properties and cell responses have been reviewed. Besides, this chapter also concentrated on the researches of development of functional graded scaffold as artificial replacement for native tissue.

Chapter 3 demonstrates the materials and scaffold fabrication method which have been used in this research. Fish skin gelatin was first dissolved in solvent in order to produce polymer solution. The solution was then electrospun into homogenous scaffolds and functional graded scaffold at designated process parameters. Three crosslinking methods which performed on the electrospun scaffolds were presented in detail. Besides that, details of characterization methods and mechanical testing which conducted on electrospun scaffolds were also introduced. Furthermore, the *in vitro* cell culture and types of testing were also described in this chapter.

Chapter 4 presents the fabrication of electrospun fish skin gelatin scaffold at different electrospinning process parameters. The influences of process parameters on fiber diameter of electrospun scaffolds have been revealed and discussed in this chapter. Moreover, this chapter also studied about the effects of fiber diameter on tensile and fracture properties of electrospun scaffolds. Observation on failure mechanism revealed in this chapter provided an understanding on the crack propagation on scaffold which consisted of different fiber diameter.

Chapter 5 discusses about the influences of crosslinking methods on electrospun fish skin gelatin scaffold's performances. After electrospun scaffolds were crosslinked with GA vapor at different conditions, *e.g.*, 5 % and 25 % of GA concentration, changes in appearance, morphology as well as topology of scaffolds were presented and discussed. Besides that, the influences of crosslinking conditions on mechanical behavior of scaffolds in terms of tensile and fracture properties were also identified and discussed in this chapter. Other than that, the swelling and degradation properties of crosslinked scaffolds were also evaluated and discussed.

Chapter 6 presents the performances assessments on two types of electrospun scaffolds which consisted of different fiber diameters. The influences of fiber diameter on *in vitro* chondrocytes proliferation, cell morphology as well as GAGs formation were assessed and discussed in this chapter. Besides that, the mechanical performances of both types of scaffolds were then compared to native soft tissues and other mechanical enhancement strategies.

Chapter 7 demonstrates the fabrication of functional graded electrospun fish skin gelatin scaffold using sequential electrospinning technique. The morphology and cross section of graded scaffold were visualized to confirm the changes of fiber diameter over the thickness. The failure mechanism of graded scaffold was also visualized under SEM. Besides that, both swelling and degradation tests were performed to access scaffold's stability in aqueous condition. In this chapter, fabrication method of functional graded scaffold was discussed. Furthermore, this chapter also discussed the mechanical performances comparison of graded scaffold with native soft tissues including articular cartilage.

Finally, Chapter 8 presents the final conclusions which drawn out based on the research findings. Some recommendations for future work also have been presented in Chapter 8.



## CHAPTER 2

### LITERATURE REVIEW

#### 2.1 Introduction to Articular Cartilage

Hyaline cartilage, fibrocartilage, elastic cartilage distinguished by their molecular components in the ECM, anatomic location and functions. Hyaline (articular) cartilage is the most abundant type of cartilage in body which can be primarily found on the articular surface of joints. It is also located at the tip of nose, trachea, larynx and costal. The articular cartilage is a smooth yet flexible connective tissue with white and glassy appearance (Mow, Ratcliffe & Poole, 1992). Its thickness ranges from a few hundred micrometres to less than 5 millimetres, depending on the location in body (Stockwell, 1971; Quinn, Hunziker & Häuselmann, 2005; Antos *et al.*, 2018; Shah *et al.*, 2019). Besides that, gender, age, weight, height as well as body mass index (BMI) also relate to influence articular cartilage thickness (Shepherd & Seedhom, 1999; Shah *et al.*, 2019; Wang & Liang, 2019). The ECM of an articular cartilage consists of tissue fluid, collagen fibers, proteoglycans and chondrocytes.

The functions of an articular cartilage including distribute load evenly and provide low friction movement. The mechanical properties of this tissue are determined at tissue length scale and these properties mainly depended on the composition and architectures of articular cartilage such as collagen fibers and proteoglycans.

### 2.1.1 Composition of articular cartilage

Generally, an articular cartilage consists of two phases: solid phase and liquid phase. The dominant components of solid phase are chondrocytes, collagens, proteoglycans and non-collagenous proteins while for the liquid phase are tissue fluid.

Tissue fluid, the most abundant component of an articular cartilage, accounts for about 60 – 85 % of its total wet weight (Mow *et al.*, 1992; Buckwalter, Mankin & Grodzinsky, 2005; Bhosale & Richardson, 2008). It is a saline based substance which abundant in hyaluronan, glycosaminoglycans (GAGs) and lubricin. As primary carrier, the tissue fluid content in articular cartilage helps in providing lubrication, distributing nutrient and oxygen to chondrocytes and transporting waste within tissue. Besides water, it also contains gases, metabolites and cations (positive ions). The presence of large number of cations within the tissue fluid is to balance the negatively charged cartilage ECM. The negatively charged in ECM arise from sulfate and carboxyl groups of proteoglycans (Mansour, 2003). The repulsive force between negative charges leads the proteoglycan molecules to diffuse and hold large volume in cartilage.

Collagen, the major constituents of solid phase of an articular cartilage, accounts for about 15 – 22 % of wet weight (Mow *et al.*, 1992) or 60 % of dry weight (Buckwalter *et al.*, 2005; Wang & Peng, 2014). The collagen fibrils embedded in cartilage responsible to tensile, tear and shear resistance (Zhang, Hu *et al.*, 2009; Both, Yang & Jansen, 2012). Collagen type II is the major type of collagen which covers about 90 – 95 % of total collagen in an adult cartilage ECM (Eyre, Weis & Wu, 2006; Responde, Natoli & Athanasiou., 2007).

In articular cartilage, another main yet unique component is proteoglycans which occupy about 4 – 7 % of total wet weight (Mow *et al.*, 1992) or 25 – 35 % of total dry weight (Buckwalter *et al.*, 2005; Wang & Peng, 2014). They help to maintain tissue fluid and electrolyte balance in an articular cartilage, in addition to provide compressive strength to the cartilage (Zhang, Hu *et al.*, 2009). These protein polysaccharide molecules are produced, maintained and secreted into the cartilage ECM by chondrocytes. A variety of proteoglycans present in cartilage, including aggrecan, decorin, biglycan, fibromodulin, lumican and prelecan (Knudson & Knudson, 2001). Among them, aggrecan is found the primary proteoglycan and

possess the largest size in articular cartilage. The functions of these proteoglycans are defined by their core protein and their glycosaminoglycans (GAGs) chains. The presence of carboxyl and sulfate groups on the aggrecan GAG have caused the proteoglycans and also cartilage ECM to be negatively charged. Because of this negative charge, the matrix has the tendency to imbibe fluid, or swelling the tissue (Landínez-Parra, Garzón-Alvarado & Vanegas-Acosta, 2012). As a result, the articular cartilage has hydrophilic properties.

Beside collagen and proteoglycans, a mature articular cartilage also contains non-collagenous proteins which occur in minute amounts. These non-collagenous proteins contribute about 15 – 20 % of total dry weight of cartilage (Buckwalter *et al.*, 2005; Wang & Peng, 2014). In addition to glycoproteins, other non-collagenous proteins commonly found in articular cartilage are included fibronectin and tenascin. However, the specific functions of these non-collagenous proteins have not been fully characterized and are currently being investigated.

In humans, chondrocyte which originates from mesenchymal stem cells (MSCs), is the only cell type present in an articular cartilage tissue, which accounts for about 1 – 5 % the volume of articular cartilage (Hunziker, Quinn & Hauselmann, 2002; Quinn *et al.*, 2005). It is a specified cell that responsible in synthesizing and remodeling/repairing highly hydrated cartilage ECM like collagen and proteoglycan *in vitro* to maintain tissue's size and mechanical properties.

### **2.1.2 Hierarchical structure of articular cartilage**

The hierarchical organization of an articular cartilage over different length scale is illustrates in Figure 2.1.

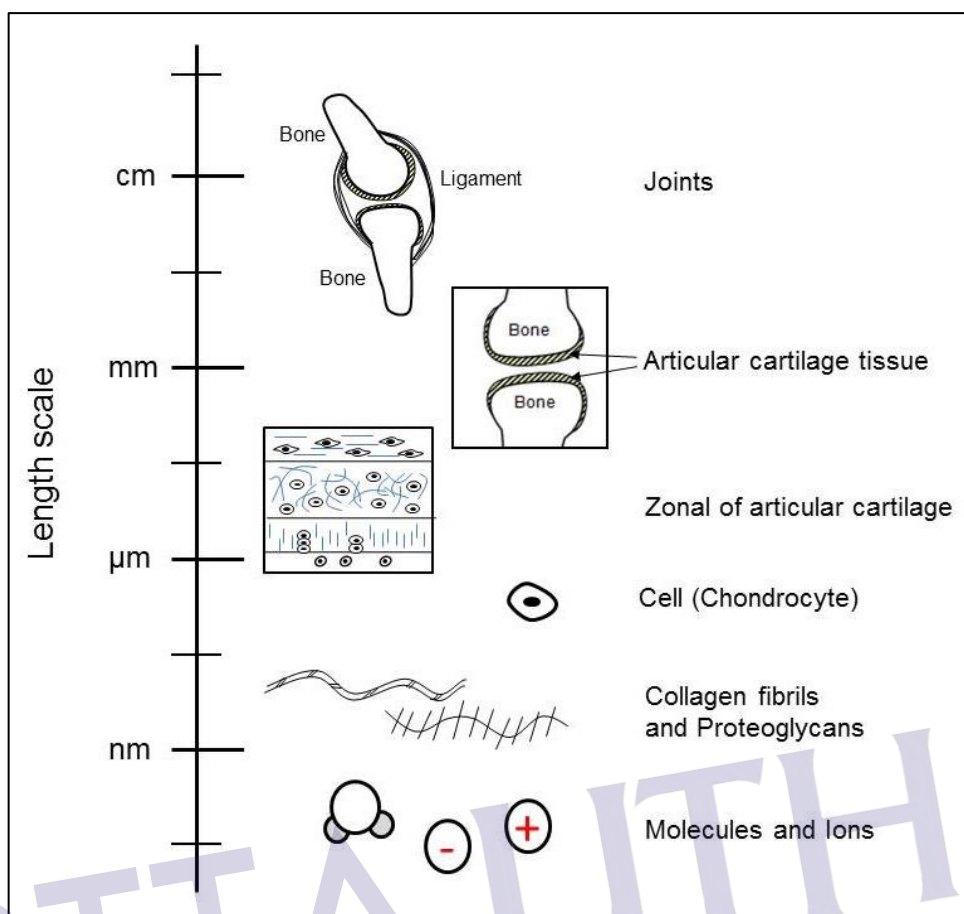


Figure 2.1: Schematic illustration of hierarchical structure of the articular cartilage over different length scale (adapted from Mow *et al.*, 1992)

At the nano structural length scale, ions, triple helix collagen molecules in collagen fibrils and glycosaminoglycans (GAGs) chains in proteoglycans are the basic building blocks of an articular cartilage hierarchy. Triple helix collagen molecules assembled to form collagen fibrils and then organized into collagen fibers. At one step further, under a scanning electron microscope, the microstructural features of the tissue such as arrangement of collagen fibers and cells can be observed. The organization of articular cartilage at this level can be divided into four different zones: superficial, transitional, deep and calcified zone. Each zone is composed of fibers arranged in different geometric pattern. The four distinct layers form few millimetres thick articular cartilage. Finally, at the largest length scale, bone, ligaments and articular cartilage are organized to form a joint with approximate 0.5 to 15 cm (Mow *et al.*, 1992).

### 2.1.3 Structure and zonal organization of articular cartilage

In designing and developing treatments for articular cartilage repair and regeneration, the knowledge of fundamental structure of this native tissue is very essential. The structure of articular cartilage is not homogenous in nature and can be divided into multiple zones, which are superficial zone, transitional zone, deep zone and calcified zone (Hwang *et al.*, 1992; Izadifar, Chen & Kulyk, 2012; Landínez-Parra *et al.*, 2012). These zones are classified based on their differences in matrix morphology (Hwang *et al.*, 1992; Changoor *et al.*, 2011), matrix composition (Mow *et al.*, 1992), cell density (Stockwell, 1967; Stockwell, 1971; Hunziker *et al.*, 2002), and metabolic properties. Each zone plays different roles within an articular cartilage. Figure 2.2 and Figure 2.3 illustrate zonal organization of collagen fibrils and chondrocytes in an articular cartilage, respectively.

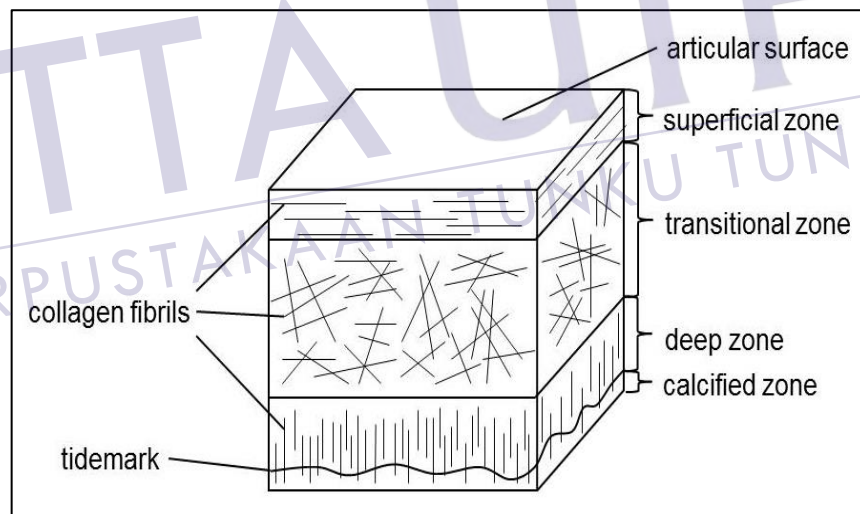


Figure 2.2: Zonal organization of collagen fibrils in an articular cartilage (adapted from Mow *et al.*, 1992).

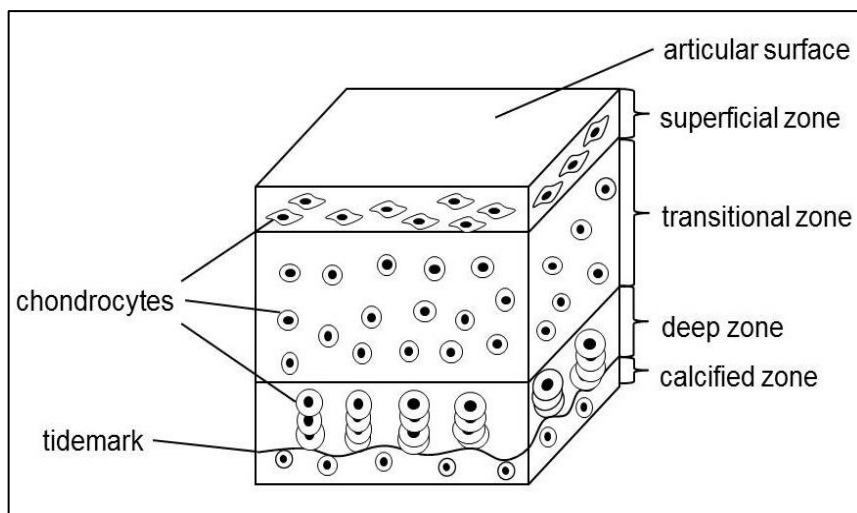


Figure 2.3: Zonal organization of chondrocytes in an articular cartilage (adapted from Mow *et al.*, 1992).

The superficial zone is the thinnest layer in articular cartilage which is about 10 – 20 % of total thickness of the tissue (Mow *et al.*, 1992; Mow, Gu & Chen, 2005). The morphology of chondrocytes in this zone is parallel to articular surface. Cell densities appeared higher than in the deeper tissue zones (Stockwell, 1967; Stockwell, 1971; Hunziker *et al.*, 2002). The activity and protein synthesis of cells are low (Landínez-Parra *et al.*, 2012). This zone contains highest concentration of fine collagen fibrils and lowest concentration of proteoglycans (Mow *et al.*, 1992; Zhang, Hu *et al.*, 2009; Fischenich *et al.*, 2020). The collagen fibrils are distributed parallel to articular surface where they are compactly arranged in groups of five to six fibrils, or showed a tendency to twist around one another (Hwang *et al.*, 1992). Chondrocytes in this zone appear in oval form, with long axis parallel to the articular surface (Hunziker *et al.*, 2002).

The transitional zone, located in between superficial and deep zone, accounts for 40 – 60 % of the total thickness of tissue (Mow *et al.*, 1992; Mow *et al.*, 2005). This zone contains higher concentration of proteoglycan and lower concentration of collagen fibrils than superficial zone (Mow *et al.*, 1992). Chondrocytes in this zone appear more rounded and randomly oriented as compared to chondrocytes in superficial zone (Hunziker *et al.*, 2002). The collagens fibrils appear in larger fiber size (Hwang *et al.*, 1992) and randomly oriented (Bhosale & Richardson; 2008; Zhang, Hu *et al.*, 2009).

The deep zone covers about 30 % of total articular cartilage thickness (Mow *et al.*, 1992; Mow *et al.*, 2005). Similar to transitional zone, the cells in deep zone are rounded but appear larger in size. The collagen fibrils located in the deep zone have the largest diameter and are perpendicular to articular surface (Weiss, Rosenberg & Helfet, 1968; Hwang *et al.*, 1992). The concentration of proteoglycan is about 15% lower than to those in the former zone while for water content is the least in this layer (Mow *et al.*, 1992; Zhang, Hu *et al.*, 2009). Cells in this layer, arranged in columns irregularly and perpendicular to articular surface (Hunziker *et al.*, 2002), shows 10 times higher synthetic activity than cells in the superficial zone (Wong *et al.*, 1996; Temenoff & Mikos, 2000; Zhang, Hu *et al.*, 2009).

The calcified zone, separated from the deep zone by a wavy plane called tidemark, is a thin mineralized layer that lies close to subchondral bone. It acts as a transition between soft hyaline cartilage and bone which minimize the stiffness gradient between rigid bone and cartilage (Izadifar *et al.*, 2012). Therefore, significant shear stress can be generated between soft cartilage and stiff bone. The orientation of collagen fibrils in this layer is just like in deep zone, which is oriented radially and arranged tightly (Hwang *et al.*, 1992; Mansour, 2003). The metabolic activity is very low since only a small number of cells, chondrocytes, are embedded. The chondrocytes here are smaller and scarce (Temenoff & Mikos, 2000). This zone is rich in hydroxyapatite crystals (Landínez-Parra *et al.*, 2012) and has same extent of calcified like bone (Wilson *et al.*, 2005). Unlike other zones, the calcified zone is the only layer contains type X collagen which replaced type II collagen. The type X collagen aids in cartilage mineralization, shock absorption along with subchondral bone and provides structural integrity (Cohen, Foster & Mow, 1998; Bhosale & Richardson, 2008).

Table 2.1 summarizes component morphology, size and composition of four distinct articular cartilage regions.

Table 2.1: Summary of component morphology, size and composition of four distinct articular cartilage regions

Cartilage component	Superficial zone	Transitional zone	Deep zone	Calcified zone	Reference(s)
Collagen fibril diameters (nm)	30 – 35	--	40 – 80	No data	Weiss <i>et al.</i> (1968)
	25 – 50	60 – 140	Up to 160	No data	Hwang <i>et al.</i> (1992)
Collagen fibre diameters (nm)	55.8 ± 9.4	87.5 ± 1.8	108.2 ± 1.8	No data	Changoor <i>et al.</i> (2011)
Water content (%)	~ 80	-	~ 65	No data	Mow <i>et al.</i> (1992), Bhosale & Richardson (2008), Zhang, Hu <i>et al.</i> (2009)
Total thickness (% of total tissue)	10 – 20	40 – 60	30	No data	Mow <i>et al.</i> (1992), Mow <i>et al.</i> (2005)

## 2.2 Biomechanical Properties of Articular Cartilage

Indeed, the biomechanical properties of articular cartilage's are complex. It can be regarded as a non-linear (*e.g.*, dependent on strain magnitude), viscoelastic (time or rate dependent), non-homogenous (different layered morphology throughout the entire thickness), and anisotropic (different properties in different direction throughout the volumes) biological composite materials. The inhomogeneity properties of such fibrous biological tissue are attributed by the layered morphology of collagen network whilst the anisotropic properties are results from orientation of collagen fibers in the tissue (Mow *et al.*, 1992; Cohen *et al.*, 1998).

During joint movement and weight bearing, the collagen fibrils, proteoglycans and other matrix components within native articular cartilage help to maintain the biomechanical properties of articular cartilage. When a load is subjected to the native tissue, the negatively charged of proteoglycans becomes closer which causes the increase of their repulsive forces and thus enhances the compressive stiffness of tissue (Mansour, 2003). Besides, not only compression stress, an articular cartilage is also experiencing to complex stress during impulsive compressive



loading, including tensile and shear. Such compressive loading has significantly generated tensile and shear stresses within the tissue. The tensile properties of articular cartilage are discussed in the following subsection.

### 2.2.1 Tensile properties of articular cartilage

In articular cartilage, the primary function of collagen fibers is to provide resistance to tensile loads. Compared to compression, tension is more likely to cause failure to the tissue. The tissue can sustain much greater strain in pure compression than in tension. No failure was found in the compression specimen at up to 50 % of compressive strain subjected whilst about 25 % of tensile specimen experienced failure at strain of 20 % or 25 % (Huang *et al.*, 2005). Hence, understanding on articular cartilage mechanical behavior in tension is essential in aiding development of artificial cartilage replacement.

As mentioned in section 2.2, articular cartilage exhibits viscoelastic characteristic in tension. Hence, the stress-strain relationship and tensile modulus are highly dependent on strain rate. Tissue will become stiffer with increasing of strain rate (Verteramo & Seedhom, 2004). This viscoelastic behavior is the result of fluid flow from tissue and internal friction related with collagen-proteoglycan molecular motion. The viscoelastic effects within the tissue will become significant as the strain rate increases. Substantial amount of tissue fluid flow out from tissue when high strain rate is applied (Roth & Mow, 1980). True volumetric changes and material properties of cartilage specimens are then difficult to access.

Therefore, in evaluating tensile properties of solid phase within the articular cartilage, it is essential to invalidate the existence of fluid flow effects. Two approaches have been implemented in previous studies to determine tensile properties of the collagen-proteoglycan solid matrix. One of the approaches is to perform a very slow strain rate (near to equilibrium) tensile experiment, typically with displacement rate of 5 mm/min (Kempson *et al.*, 1973; Kempson, 1982), to avoid significant flow generated stiffening effect and thus measure tensile modulus. Another method is performing the tensile experiment with stress relaxation to allow

the specimen reaches equilibrium at each strain increment. Through both approaches, the mechanical properties of solid matrix can be determined.

From previous works, it can be noted that only a range of values, no specific value for tensile properties of articular cartilage obtained even though different studies have been conducted to determine these properties. This variation arises from numbers of factors (Roth & Mow, 1980; Akizuki *et al.* 1986; Charlebois, McKee & Buschmann, 2004; Huang *et al.*, 2005; Oinas *et al.*, 2018), including type of species, age of species, type of joints taken in the species, region in the joint (*e.g.*, high load weight bearing area or low load weight bearing area), and state of degradation. Akizuki and coworkers (1986) reported that the stress strain behavior of normal human articular cartilage is linear up to 15 % strain. They also found that the tensile modulus was less than 30 MPa, most in the range between 1 MPa to 15 MPa.

Typically, as with other soft collagenous biological tissues, the articular cartilage also indicates nonlinear tensile behavior. Figure 2.4 is a schematic representation of a stress-strain curve of an articular cartilage, showing a nonlinear tensile behavior. As shown in the figure, there is a nonlinear and a linear region before cartilage fails. The nonlinear 'toe region' indicates that the native tissue deforms easily when there is a small load subjected on it. Small load acting on it causes a large deformation. This is due to the initial state of fibrous collagen network within the tissue where collagen fibers are not particularly stretched. Tensile load is required to slip collagen fibers through the gel like proteoglycan initially. When the collagen fibers are eventually stretched, they will start to absorb the tensile load acting on them. The tissue will then become stiffer as strain increased, as indicated in linear region of Figure 2.4. Actual stiffness and strength of collagen fibers network is observed in this region.

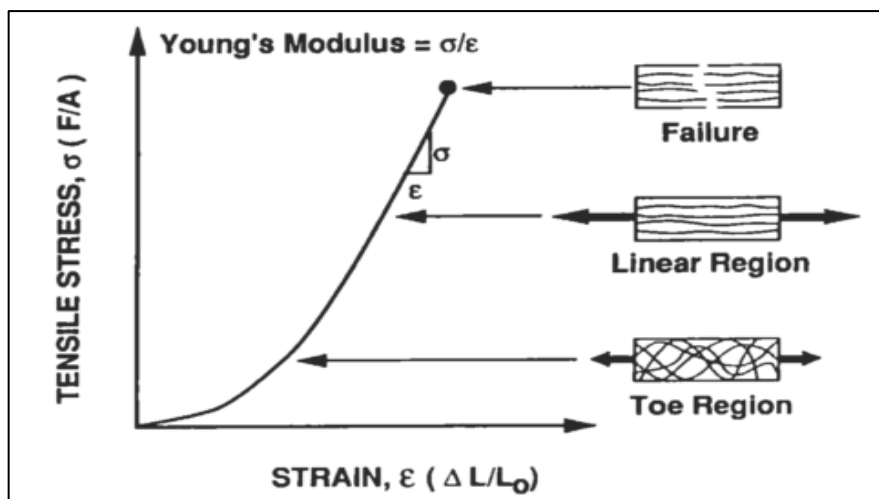


Figure 2.4: Stress-strain curve of an articular cartilage, showing nonlinear tensile behavior (Cohen *et al.*, 1998).

Sasazaki, Shore & Seedhom (2006) observed the deformation and failure mechanism of bovine cartilage in tensile mode. A systematic investigation towards the cartilage failure when tensile strain was subjected has been carried out from macroscopic level to the ultrastructural level. Through their observation, matrix reorganization (collagen meshwork and chondrocytes) occurred before failure. When tensile strain was 0 %, the fibrillar meshwork within articular surface was predominantly orientated. Collagen in the articular surface reorganized and aligned to direction of applied strain when strain was increased from 0 %. About 3  $\mu\text{m}$  in diameter of ridges bundle, parallel to the applied strain direction, was observed on the articular surface. Mansfield and coworkers (2015) also reported similar observation on surface corrugation on superficial zone of horses' cartilage at high strains. After the fibrillar meshwork was completely reoriented and aligned to the applied strain direction, cartilage failure was initiated with the rupture of fibrillar meshwork within the articular surface. Finally, failure of cartilage was completed with the rapid propagated rupture of subjacent layers throughout full thickness of cartilage.

### 2.2.1.1 Zonal variations of articular cartilage in mechanical properties

Owing to variation in the articular cartilage's structure and composition in each zonal, the mechanical forces acting on the tissue are different. These mechanical differences of this tissue are attributed by the variation of cells (morphology, density, orientation and metabolic activity), collagen fibrils (diameter, density and orientation) and GAGs (type and amount) over the depth of the articular cartilage (Hu & Athanasiou, 2003).

As discussed in previous section, arrangement of collagen fibril within the ECM of articular cartilage is non-homogenous and anisotropic. The inhomogeneity of cartilage is associated to the layered morphology of collagen network whereas the anisotropy is related to the collagen fibres orientation within the tissue (Mow *et al.*, 1992). Starting from superficial zone which has the orientation of collagen fibrils parallel to the articular surface, the collagen fibrils orientation changes through transition zone to deep zone and tidemark where the collagen fibrils oriented normal to articular surface. Because of the orientation and collagen fibrils diameters are different at each zone, therefore the mechanical properties vary from zone to zone. Table 2.2 states the mechanical properties of each zone obtained from previous studies.

Table 2.2: Zonal variations in mechanical properties of human articular cartilage

Mechanical properties	Superficial zone	Transitional zone	Deep zone	Calcified zone	Reference(s)
Tensile modulus (MPa)	20.67 ± 3.01 <sup>a</sup>	4.14 ± 1.72 <sup>a</sup>	No data	No data	Akizuki <i>et al.</i> (1986)
	10.13 ± 1.78 <sup>b</sup>	4.54 ± 1.28 <sup>b</sup>	No data	No data	
Ultimate strain	~ 0.20	No data	~ 0.45	No data	Bader <i>et al.</i> (1981)
Poisson's ratio	1.87 ± 1.11 <sup>c</sup>	0.62 ± 0.23 <sup>c</sup>	No data	No data	Elliott, Narmoneva & Setton (2002)

location = <sup>a</sup> lateral patella groove, <sup>b</sup> medial femoral condyle, <sup>c</sup> patella

From table above and findings from previous studies, some general conclusions may be made. Superficial zone exhibits highest tensile stiffness among

other zones (Kempson, Freeman & Swanson, 1968; Akizuki *et al.*, 1986, Bell *et al.*, 2014). The tensile stiffness of native articular cartilage tissue was found to be decreased as distance from the articular surface increased (Kempson *et al.*, 1968; Kempson *et al.*, 1973; Akizuki *et al.*, 1986; Mow *et al.*, 2005). At higher strain and tensile loading, superficial zone tends to reorganize. Surface corrugation and ridges bundle were observed (Sasazaki *et al.*, 2006; Mansfield *et al.*, 2015). Hence, it is believed that such changes are to resist deformation and failure of superficial zone. Once the superficial layer loss its stiffness and failure, the remaining lower zones will subject rapid degeneration process (Akizuki *et al.*, 1986; Sasazaki *et al.*, 2006).

### 2.2.2 Fracture of articular cartilage

Cracks appeared in the articular cartilage due to trauma, wear and tear or when the joint is forced to exceed its normal range of motion periodically. Owing to various causes such as sudden high forces, fatigue, creep and *etc.*, cracks can grow very rapidly and can cause pain which compromises the knee movement. As the crack size increases, the failure strength of tissue decreases. Over a period of time, the failure strength becomes very low and thus the tissue may fail in service. Once the tissue exhibits defects, it has poor healing ability due to their avascular nature. Hence, articular cartilage must exhibit sufficient toughness to resist the propagation of defects *in vivo*.

The failure properties of articular cartilage with presence of crack have to be evaluated by fracture toughness technique. Fracture toughness is an important material property to describe defect tolerance of a material. It measures the ability of a material to resist the cracks propagation. Under a modified single edge notched test (MSEN), the fracture toughness of normal articular cartilage was about 0.14 – 1.2 kN/m (Chin-Purcell & Lewis, 1996).

Figure 2.5 shows five stages of crack growth mechanism in an articular cartilage. As shown in the figure, a micro-crack appeared in the tissue may eventually result failure to the tissue under tensile loading. Instead of expanding towards the bottom layer of the tissue, the crack grew in a stretching manner in the loading direction and parallel to the articular surface. The curve illustrated in the

Figure 2.5 also revealed that the tissue exhibits brittle fracture (when stage 4 is negligible) or initial brittle fracture followed by a period of steady crack growth before sudden fracture. This indicates that in evaluating the fracture mechanics of articular cartilage, it is possible to describe the cartilage fracture in linear elastic fracture mechanics (Stok & Oloyede, 2007).

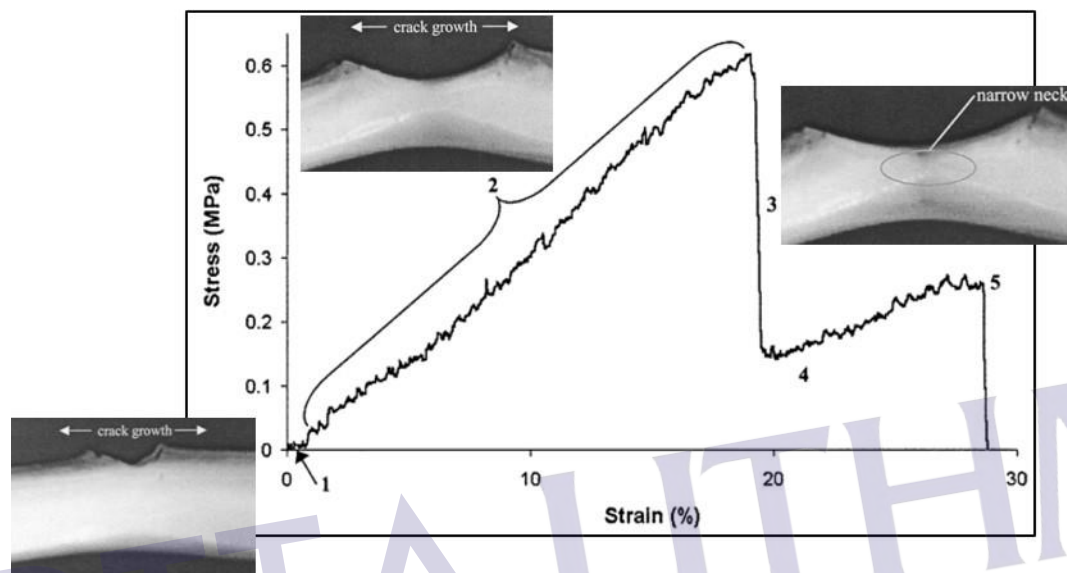


Figure 2.5: Five stages of crack growth in articular cartilage (Stok & Oloyede, 2003).

As illustrated in Figure 2.5, Stok and Oloyede (2003) suggested that the fracture propagation of an articular cartilage has five stages at any strain rate, which are:

1. Initial rapid opening by stretching along the loading direction.
2. Prolonged stable opening, by stretching, of the articular surface. The rapid opening was slowed down into a stable growth phase. Deep matrix was pulled up towards the crack root. This region indicated the superb toughness of articular cartilage.
3. Rapid necking and unstable growth of the general matrix.
4. A temporary cessation of unstable propagation, followed by a brief period of stable propagation. In some cases, stage 3 was followed by stage 5, skipping the stage 4.

## REFERENCES

Agheb, M., Dinari, M., Rafienia, M., & Salehi, H. (2017). Novel electrospun nanofibers of modified gelatin-tyrosine in cartilage tissue engineering. *Materials Science and Engineering C*, 71, 240 – 251.

Agrawal, A., Rahbar, N., & Calvert, P. D. (2013). Strong fiber-reinforced hydrogel. *Acta Biomaterialia*, 9(2), 5313 – 5318.

Akizuki, S., Mow, V. C., Müller, F., Pita, J. C., Howell, D. S., & Manicourt, D. H. (1986). Tensile properties of human knee joint cartilage: I. Influence of ionic conditions, weight bearing, and fibrillation on the tensile modulus. *Journal of Orthopaedic Research: Official Publication of the Orthopaedic Research Society*, 4(4), 379 – 392.

Amadori, S., Torricelli, P., Rubini, K., Fini, M., Panzavolta, S., & Bigi, A. (2015). Effect of sterilization and crosslinking on gelatin films. *Journal of Materials Science: Materials in Medicine*, 26(2), 69.

An, K., Liu, H., Guo, S., Kumar, D. N. T., & Wang, Q. (2010). Preparation of fish gelatin and fish gelatin/poly(l-lactide) nanofibers by electrospinning. *International Journal of Biological Macromolecules*, 47(3), 380 – 388.

Antich, C., de Vicente, J., Jiménez, G., Chocarro, C., Carrillo, E., Montañez, E., Gálvez-Martín, P., & Marchal, J. A. (2020). Bio-inspired hydrogel composed of hyaluronic acid and alginate as a potential bioink for 3D bioprinting of articular cartilage engineering constructs. *Acta Biomaterialia*, 106, 114 – 123.

Antons, J., Marascio, M. G. M., Nohava, J., Martin, R., Applegate, L. A., Bourban, P. E., & Pioletti, D. P. (2018). Zone-dependent mechanical properties of human articular cartilage obtained by indentation measurements. *Journal of Materials Science: Materials in Medicine*, 29(5), 1 – 8.

Athanasίου, K. A., Darling, E. M., Hu, J. C., DuRaine, G. D., & Reddi, A. H. (2013). *Articular cartilage*. CRC Press: Taylor and Francis Group.

Bader, D. L., Kempson, G. E., Barrett, A. J., & Webb, W. (1981). The effects of proteoglycan degradation on the mechanical properties adult human articular cartilage in tension. *Biochimica et Biophysica Acta*, 677, 103 – 108.

Baji, A., Mai, Y. W., Wong, S. C., Abtahi, M., & Chen, P. (2010). Electrospinning of polymer nanofibers: Effects on oriented morphology, structures and tensile properties. *Composites Science and Technology*, 70(5), 703 – 718.

Bashur, C. A., Dahlgren, L. A., & Goldstein, A. S. (2006). Effect of fiber diameter and orientation on fibroblast morphology and proliferation on electrospun poly(D,L-lactic-co-glycolic acid) meshes. *Biomaterials*, 27(33), 5681 – 5688.

Beachley, V., & Wen, X. (2009). Effect of electrospinning parameters on the nanofiber diameter and length. *Materials Science and Engineering: C*, 29(3), 663 – 668.

Bean, A. C., & Tuan, R. S. (2015). Fiber diameter and seeding density influence chondrogenic differentiation of mesenchymal stem cells seeded on electrospun poly( $\epsilon$ -caprolactone) scaffolds. *Biomedical Materials*, 10(1), 015018.

Bell, J. S., Christmas, J., Mansfield, J. C., Everson, R. M., & Winlove, C. P. (2014). Micromechanical response of articular cartilage to tensile load measured using nonlinear microscopy. *Acta Biomaterialia*, 10(6), 2574 – 2581.



Benya, P. D., Padilla, S. R., & Nimni, M. E. (1978). Independent regulation of collagen types by chondrocytes during the loss of differentiated function in culture. *Cell*, 15(4), 1313 – 1321.

Bhardwaj, N., & Kundu, S. C. (2010). Electrospinning: A fascinating fiber fabrication technique. *Biotechnology Advances*, 28(3), 325 – 347.

Bhosale, A. M., & Richardson, J. B. (2008). Articular cartilage: structure, injuries and review of management. *British medical bulletin*, 87(1), 77 – 95.

Bigi, A., Cojazzi, G., Panzavolta, S., Roveri, N., and Rubini, K. (2002). Stabilization of gelatin films by crosslinking with genipin. *Biomaterials*, 23(24), 4827 – 4832.

Bigi, A., Cojazzi, G., Panzavolta, S., Rubini, K., and Roveri, N. (2001). Mechanical and thermal properties of gelatin films at different degrees of glutaraldehyde crosslinking. *Biomaterials*, 22(8), 763 – 768.

Bittner, S. M., Smith, B. T., Diaz-Gomez, L., Hudgins, C. D., Melchiorri, A. J., Scott, D. W., Fisher, J. P., & Mikos, A. G. (2019). Fabrication and mechanical characterization of 3D printed vertical uniform and gradient scaffolds for bone and osteochondral tissue engineering. *Acta Biomaterialia*, 90, 37 – 48.

Both, S. K., Yang, F., & Jansen, J. A. (2012). Endochondral Bone Tissue Engineering. In: Ramalingam, M., Haidar, Z., Ramakrishna S., Kobayashi, H. & Haikel, Y. (Eds.). *Integrated Biomaterials in Tissue Engineering*. Salem, MA: Scrivener Publishing. 165 – 182.

Buckwalter, J. A., Mankin, H. J., & Grodzinsky, A. J. (2005). Articular cartilage and osteoarthritis. *Instructional Course Lectures-American Academy of Orthopaedic Surgeons*, 54, 465 – 480.

Butcher, A. L., Koh, C. T., & Oyen, M. L. (2017). Systematic mechanical evaluation of electrospun gelatin meshes. *Journal of the Mechanical Behavior of Biomedical Materials*, 69, 412 – 419.

Camarero-Espinosa, S., Rothen-Rutishauser, B., Weder, C., & Foster, E. J. (2016). Directed cell growth in multi-zonal scaffolds for cartilage tissue engineering. *Biomaterials*, 74, 42 – 52.

Campiglio, C. E., Ponzini, S., De Stefano, P., Ortoleva, G., Vignati, L., & Draghi, L. (2020). Cross-Linking Optimization for Electrospun Gelatin: Challenge of Preserving Fiber Topography. *Polymers*, 12(11), 2472.

Can-Herrera, L. A., Oliva, A. I., Dzul-Cervantes, M. A. A., Pacheco-Salazar, O. F., & Cervantes-Uc, J. M. (2021). Morphological and Mechanical Properties of Electrospun Polycaprolactone Scaffolds: Effect of Applied Voltage. *Polymers*, 13(4), 662 – 672.

Cha, D. Il, Kim, K. W., Chu, G. H., Kim, H. Y., Lee, K. H., & Bhattarai, N. (2006). Mechanical behaviors and characterization of electrospun polysulfone/polyurethane blend nonwovens. *Macromolecular Research*, 14(3), 331 – 337.

Changoor, A., Nelea, M., Méthot, S., Tran-Khanh, N., Chevrier, A., Restrepo, A. Shive, M. S., Hoemann, C. D., & Buschmann, M. D. (2011). Structural characteristics of the collagen network in human normal, degraded and repair articular cartilages observed in polarized light and scanning electron microscopies. *Osteoarthritis and Cartilage*, 19(12), 1458 – 1468.

Charlebois, M., McKee, M. D., & Buschmann, M. D. (2004). Nonlinear tensile properties of bovine articular cartilage and their variation with age and depth. *Journal of Biomechanical Engineering*, 126(2), 129 – 137.

Chen, M., Patra, P. K., Warner, S. B., & Bhowmick, S. (2007). Role of Fiber Diameter in Adhesion and Proliferation of NIH 3T3 Fibroblast on Electrospun Polycaprolactone Scaffolds. *Tissue Engineering*, 13(3), 579 – 587.

Chen, Z., Wei, B., Mo, X., Lim, C. T., Ramakrishna, S., & Cui, F. (2009). Mechanical properties of electrospun collagen-chitosan complex single fibers and membrane. *Materials Science and Engineering C*, 29(8), 2428 – 2435.

Chin-Purcell, M. V., & Lewis, J. L. (1996). Fracture of Articular Cartilage. *Journal of Biomechanical Engineering*, 118(4), 545 – 556.

Chiou, B-S., Avena-Bustillos, R. J., Bechtel, P. J., Jafri, H., Narayan, R., Imam, S. H., Glenn, G. M., & Orts, W. J. (2008). Cold water fish gelatin films: Effects of cross-linking on thermal, mechanical, barrier and biodegradation properties. *European Polymer Journal*, 44(11), 3748 – 3753.

Choktaweessap, N., Arayanarakul, K., Aht-ong, D., Meechaisue, C., & Supaphol, P. (2007). Electrospun Gelatin Fibers: Effect of Solvent System on Morphology and Fiber Diameters. *Polymer Journal*, 39(6), 622 – 631.

Christopherson, G. T., Song, H., & Mao, H. Q. (2009). The influence of fiber diameter of electrospun substrates on neural stem cell differentiation and proliferation. *Biomaterials*, 30(4), 556 – 564.

Coburn, J. M., Gibson, M., Monagle, S., Patterson, Z., & Elisseeff, J. H. (2012). Bioinspired nanofibers support chondrogenesis for articular cartilage repair. *Proceedings of the National Academy of Sciences*, 109(25), 10012 – 10017.

Cohen, N. P., Foster, R. J., & Mow, V. C. (1998). Composition and dynamics of articular cartilage: structure, function, and maintaining healthy state. *Journal of Orthopaedic & Sports Physical Therapy*, 28(4), 203 – 215.

Coimbra, P., Gil, M. H., & Figueiredo, M. (2014). Tailoring the properties of gelatin films for drug delivery applications: Influence of the chemical cross-linking method. *International Journal of Biological Macromolecules*, 70, 10 – 19.

Cooke, M. E., Lawless, B. M., Jones, S. W., & Grover, L. M. (2018). Matrix degradation in osteoarthritis primes the superficial region of cartilage for mechanical damage. *Acta Biomaterialia*, 78, 320–328.

De Schoenmaker, B., Van der Schueren, L., Ceylan, Ö., & De Clerck, K. (2012). Electrospun Polyamide 4.6 Nanofibrous Nonwovens: Parameter Study and Characterization. *Journal of Nanomaterials*, 2012, 1 – 9.

De Silva, D. A., Martens, P. J., Gilmore, K. J., & Panhuis, M. In Het. (2014). Degradation behavior of ionic-covalent entanglement hydrogels. *Journal of Applied Polymer Science*, 132(1), 1 – 10.

De Vrieze, S., Van Camp, T., Nelvig, A., Hagström, B., Westbroek, P., & De Clerck, K. (2009). The effect of temperature and humidity on electrospinning. *Journal of Materials Science*, 44(5), 1357 – 1362.

Deitzel, J. M., Kleinmeyer, J., Harris, D., & Beck Tan, N. C. (2001). The effect of processing variables on the morphology of electrospun nanofibers and textiles. *Polymer*, 42(1), 261 – 272.

Demir, M., Yilgor, I., Yilgor, E., & Erman, B. (2002). Electrospinning of polyurethane fibers. *Polymer*, 43(11), 3303 – 3309.

Davidenko, N., Schuster, C. F., Bax, D. V., Raynal, N., Farndale, R. W., Best, S. M., & Cameron, R. E. (2015). Control of crosslinking for tailoring collagen-based scaffolds stability and mechanics. *Acta Biomaterialia*, 25, 131 – 142.

Di Luca, A., Ostrowska, B., Lorenzo-Moldero, I., Lapedda, A., Swieszkowski, W., Van Blitterswijk, C., & Moroni, L. (2016). Gradients in pore size enhance the osteogenic differentiation of human mesenchymal stromal cells in three-dimensional scaffolds. *Scientific Reports*, 6(1), 22898.

Di Luca, A., Szlazak, K., Lorenzo-Moldero, I., Ghebes, C. A., Lapedda, A., Swieszkowski, W., Van Blitterswijk, C., & Moroni, L. (2016). Influencing chondrogenic differentiation of human mesenchymal stromal cells in scaffolds displaying a structural gradient in pore size. *Acta Biomaterialia*, 36, 210 – 219.

Eichhorn, S. J., & Sampson, W. W. (2005). Statistical geometry of pores and statistics of porous nanofibrous assemblies. *Journal of the Royal Society Interface*, 2(4), 309 – 318.

Elliott, D. M., Narmoneva, D. A., & Setton, L. A. (2002). Direct Measurement of the Poisson's Ratio of Human Patella Cartilage in Tension. *Journal of Biomechanical Engineering*, 124(2), 223 – 228.

Erisken, C., Zhang, X., Moffat, K. L., Levine, W. N., & Lu, H. H. (2013). Scaffold fiber diameter regulates human tendon fibroblast growth and differentiation. *Tissue Engineering - Part A*, 19(3–4), 519 – 528.

Eyre, D. R., Weis, M. A., & Wu, J. J. (2006). Articular cartilage collagen: an irreplaceable framework? *European cells & materials*, 12(1), 57 – 63.

Fashandi, H. & Karimi, M. (2012). Pore formation in polystyrene fiber by superimposing temperature and relative humidity of electrospinning atmosphere. *Polymer*, 53(25), 5832 – 5849.

Ferreira, J. L., Gomes, S., Henriques, C., Borges, J. P., & Silva, J. C. (2014). Electrospinning polycaprolactone dissolved in glacial acetic acid: Fiber production, nonwoven characterization, and In Vitro evaluation. *Journal of Applied Polymer Science*, 131(22), 41068.

Fischenich, K. M., Wahlquist, J. A., Wilmoth, R. L., Cai, L., Neu, C. P., & Ferguson, V. L. (2020). Human articular cartilage is orthotropic where microstructure, micromechanics, and chemistry vary with depth and split-line orientation. *Osteoarthritis and Cartilage*, 28(10), 1362 – 1372.

Fong, H., Chun, I., & Reneker, D. (1999). Beaded nanofibers formed during electrospinning. *Polymer*, 40(16), 4585 – 4592.

Furuike, T., Chaochai, T., Okubo, T., Mori, T., & Tamura, H. (2016). Fabrication of nonwoven fabrics consisting of gelatin nanofibers cross-linked by glutaraldehyde or N-acetyl-D-glucosamine by aqueous method. *International Journal of Biological Macromolecules*, 93, 1530 – 1538.

Gao, S., Yuan, Z., Guo, W., Chen, M., Liu, S., Xi, T., & Guo, Q. (2017). Comparison of glutaraldehyde and carbodiimides to crosslink tissue engineering scaffolds fabricated by decellularized porcine menisci. *Materials Science and Engineering C*, 71, 891 – 900.

Gholipour Kanani, A., & Bahrami, S. H. (2011). Effect of Changing Solvents on Poly(-Caprolactone) Nanofibrous Webs Morphology. *Journal of Nanomaterials*, 2011(724153), 1 – 10.

Gomes, D. S., Silva, A. N. R. da, Morimoto, N. I., Mendes, L. T. F., Furlan, R., & Ramos, I. (2007). Characterization of an electrospinning process using different PAN/DMF concentrations. *Polímeros*, 17(3), 206 – 211.

Gomes, S. R., Rodrigues, G., Martins, G. G., Henriques, C. M. R., & Silva, J. C. (2013). In vitro evaluation of crosslinked electrospun fish gelatin scaffolds. *Materials Science and Engineering C*, 33(3), 1219 – 1227.

Gomes, S. R., Rodrigues, G., Martins, G. G., Roberto, M.A., Mafra, M., Henriques, C. M. R., & Silva, J. C. (2015). In vitro and in vivo evaluation of electrospun nanofibers of PCL, chitosan and gelatin: A comparative study. *Materials Science and Engineering: C*, 46, 348 – 358.

Gómez-Guillén, M. C., Pérez-Mateos, M., Gómez-Estaca, J., López-Caballero, E., Giménez, B., & Montero, P. (2009). Fish gelatin: a renewable material for developing active biodegradable films. *Trends in Food Science & Technology*, 20(1), 3 – 16.

Gong, J. P. (2010). Why are double network hydrogels so tough? *Soft Matter*, 6(12), 2583 – 2590.

Gong, J. P., Katsuyama, Y., Kurokawa, T., & Osada, Y. (2003). Double-Network Hydrogels with Extremely High Mechanical Strength. *Advanced Materials*, 15(14), 1155 – 1158.

Grey, C. P., Newton, S. T., Bowlin, G. L., Haas, T. W., & Simpson, D. G. (2013). Gradient fiber electrospinning of layered scaffolds using controlled transitions in fiber diameter. *Biomaterials*, 34(21), 4993 – 5006.

Gu, S. Y., Ren, J., & Vancso, G. J. (2005). Process optimization and empirical modeling for electrospun polyacrylonitrile (PAN) nanofiber precursor of carbon nanofibers. *European Polymer Journal*, 41(11), 2559 – 2568.

Gu, S.-Y., Wang, Z.-M., Ren, J., & Zhang, C.-Y. (2009). Electrospinning of gelatin and gelatin/poly(l-lactide) blend and its characteristics for wound dressing. *Materials Science and Engineering: C*, 29(6), 1822 – 1828.

Guarino, V., Alvarez-Perez, M., Cirillo, V., & Ambrosio, L. (2011). hMSC interaction with PCL and PCL/gelatin platforms: A comparative study on films and electrospun membranes. *Journal of Bioactive and Compatible Polymers*, 26(2), 144 – 160.

Haque, M. A., Kurokawa, T., & Gong, J. P. (2012). Super tough double network hydrogels and their application as biomaterials. *Polymer*, 53(9), 1805 – 1822.

Harris, J. D., & Flanigan, D. C. (2011). Management of Knee Articular Cartilage Injuries. In: Dragoo, J. L. *Modern Arthroscopy*. BoD – Books on Demand. 103 – 128.

Hayat, M. E. (Ed.). (2012). *Fixation for electron microscopy*. Elsevier.

Heydarkhan-Hagvall, S., Schenke-Layland, K., Dhanasopon, A. P., Rofail, F., Smith, H., Wu, B. M., Shemin, R., Beygui, R. E., & MacLellan, W. R. (2008). Three-dimensional electrospun ECM-based hybrid scaffolds for cardiovascular tissue engineering. *Biomaterials*, 29(19), 2907 – 2914.

Homayoni, H., Ravandi, S. A. H., & Valizadeh, M. (2009). Electrospinning of chitosan nanofibers: Processing optimization. *Carbohydrate Polymers*, 77(3), 656 – 661.

Hosseini, S. A., Mohammadi, R., Noruzi, S., Ganji, R., Oroojalian, F., & Sahebkar, A. (2021). Evolution of hydrogels for cartilage tissue engineering of the knee: A systematic review and meta-analysis of clinical studies. *Joint Bone Spine*, 88(1), 105096.

Hu, J. C. Y., & Athanasiou, K. A. (2003). Structure and function of articular cartilage. In: An, Y. H. and Martin, K. L. *Handbook of histology methods for bone and cartilage*. New York: Springer Science and Business Media. 73 – 95.

Huang, C. Y., Stankiewicz, A., Ateshian, G. A., & Mow, V. C. (2005). Anisotropy, inhomogeneity, and tension-compression nonlinearity of human glenohumeral cartilage in finite deformation. *Journal of Biomechanics*, 38(4), 799 – 809.

Huang, L., Huang, J., Shao, H., Hu, X., Cao, C., Fan, S., Song, L., & Zhang, Y. (2019). Silk scaffolds with gradient pore structure and improved cell infiltration performance. *Materials Science and Engineering: C*, 94, 179 – 189.

Huang, Z. M., Zhang, Y. Z., Ramakrishna, S., & Lim, C. T. (2004). Electrospinning and mechanical characterization of gelatin nanofibers. *Polymer*, 45(15), 5361 – 5368.

Hunziker, E.B., Quinn, T.M., & Hauselmann, H. (2002). Quantitative structural organization of normal adult human articular cartilage. *Osteoarthritis and Cartilage*, 10(7), 564 – 572.

Hwang, W. S., Li, B., Jin, L. H., Ngo, K., Schachar, N. S., & Hughes, G. N. F. (1992). Collagen fibril structure of normal, aging, and osteoarthritic cartilage. *The Journal of Pathology*, 167(4), 425 – 433.



Izadifar, Z., Chen, X., & Kulyk, W. (2012). Strategic design and fabrication of engineered scaffolds for articular cartilage repair. *Journal of functional biomaterials*, 3(4), 799 – 838.

Ju, Y. M., Choi, J. S., Atala, A., Yoo, J. J., & Lee, S. J. (2010). Bilayered scaffold for engineering cellularized blood vessels. *Biomaterials*, 31(15), 4313 – 4321.

Kamata, H., Akagi, Y., Kayasuga-Kariya, Y., Chung, U. Il., & Sakai, T. (2014). “Nonswellable” hydrogel without mechanical hysteresis. *Science*, 343(6173), 873 – 875.

Kapoor, S., & Kundu, S. C. (2016). Silk protein-based hydrogels: Promising advanced materials for biomedical applications. *Acta Biomaterialia*, 31, 17 – 32.

Karim, A., Amin, A. K., & Hall, A. C. (2018). The clustering and morphology of chondrocytes in normal and mildly degenerate human femoral head cartilage studied by confocal laser scanning microscopy. *Journal of Anatomy*, 232(4), 686 – 698.

Karim, A. A., & Bhat, R. (2009). Fish gelatin: properties, challenges, and prospects as an alternative to mammalian gelatins. *Food Hydrocolloids*, 23(3), 563 – 576.

Kempson, G. E. (1982). Relationship between the tensile properties of articular cartilage from the human knee and age. *Annals of the Rheumatic Diseases*, 41(5), 508 – 511.

Kempson, G. E., Freeman, M. A. R., & Swanson, S. A. V. (1968). Tensile properties of articular cartilage. *Nature*, 220(5172), 1127 – 1128.

Kempson, G., Muir, H., Pollard, C., & Tuke, M. (1973). The tensile properties of the cartilage of human femoral condyles related to the content of collagen and glycosaminoglycans. *Biochimica et Biophysica Acta (BBA) - General Subjects*, 297(2), 456 – 472.

Kerscher, P., Kaczmarek, J. A., Head, S. E., Ellis, M. E., Seeto, W. J., Kim, J., Bhattacharya, S., Suppiramaniam, V., & Lipke, E. A. (2017). Direct Production of Human Cardiac Tissues by Pluripotent Stem Cell Encapsulation in Gelatin Methacryloyl. *ACS Biomaterials Science & Engineering*, 3(8), 1499 – 1509.

Keun Kwon, I., Kidoaki, S., & Matsuda, T. (2005). Electrospun nano- to microfiber fabrics made of biodegradable copolyesters: structural characteristics, mechanical properties and cell adhesion potential. *Biomaterials*, 26(18), 3929 – 3939.

Ki, C. S., Baek, D. H., Gang, K. D., Lee, K. H., Um, I. C., & Park, Y. H. (2005). Characterization of gelatin nanofiber prepared from gelatin-formic acid solution. *Polymer*, 46(14), 5094 – 5102.

Kim, H. H., Kim, M. J., Ryu, S. J., Ki, C. S., & Park, Y. H. (2016). Effect of fiber diameter on surface morphology, mechanical property, and cell behavior of electrospun poly( $\epsilon$ -caprolactone) mat. *Fibers and Polymers*, 17(7), 1033 – 1042.

Kirchmayer, D. M., & Panhuis, M. in het. (2014). Robust biopolymer based ionic-covalent entanglement hydrogels with reversible mechanical behaviour. *Journal of Materials Chemistry B*, 2(29), 4694 – 4702.

Knudson, C. B., & Knudson, W. (2001). Cartilage proteoglycans, *Seminars in Cell and Developmental Biology*, 12(2), 69 – 78.

Ko, J. H., Yin, H., An, J., Chung, D. J., Kim, J.-H., Lee, S. B., & Pyun, D. G. (2010). Characterization of cross-linked gelatin nanofibers through electrospinning. *Macromolecular Research*, 18(2), 137 – 143.

Koh, C. T., Low, C. Y., & Yusof, Y. (2015). Structure-property relationship of bio-inspired fibrous materials. *Procedia Computer Science*, 76, 411 – 416.

Koh, C. T., & Oyen, M. L. (2012). Branching toughens fibrous networks. *Journal of the Mechanical Behavior of Biomedical Materials*, 12, 74 – 82.

Koh, C. T., & Oyen, M. L. (2015). Toughening in electrospun fibrous scaffolds. *APL Materials*, 3(1), 014908.

Koh, C. T., Strange, D. G. T., Tonsomboon, K., & Oyen, M. L. (2013). Failure mechanisms in fibrous scaffolds. *Acta Biomaterialia*, 9(7), 7326 – 7334.

Koh, C. T., Tonsomboon, K., & Oyen, M. L. (2019). Fracture toughness of human amniotic membranes. *Interface focus*, 9(5), 20190012.

Kuo, C. K., Li, W.-J., & Tuan, R. S. (2012). Cartilage and Ligament Tissue Engineering: Biomaterials, Cellular Interactions, and Regenerative Strategies. In Ratner, B. D., Hoffman, A. S., Schoen, F. J. & Lemons, J. E. *Biomaterials Science: An Introduction to Materials in Medicine* (Third Edition). Academic Press, 1214 – 1236.

Kwak, H. W., Shin, M., Lee, J. Y., Yun, H., Song, D. W., Yang, Y., Shin, B-S., Park, Y. H., & Lee, K. H. (2017). Fabrication of an ultrafine fish gelatin nanofibrous web from an aqueous solution by electrospinning. *International journal of biological macromolecules*, 102, 1092 – 1103.

Kwon, H., Brown, W. E., Lee, C. A., Wang, D., Paschos, N., Hu, J. C., & Athanasiou, K. A. (2019). Surgical and tissue engineering strategies for articular cartilage and meniscus repair. *Nature Reviews Rheumatology*, 15(9), 550 – 570.

Landínez-Parra, N. S., Garzón-Alvarado, D. A. & Vanegas-Acosta, J. C. (2012). Mechanical Behavior of Articular Cartilage. In: Goswami, T. (Ed.). *Injury and Skeletal Biomechanics*. BoD – Books on Demand. 197 – 216.

Langer, R., & Vacanti, J. P. (1993). Tissue engineering. *Science*, 260(5110), 920 – 926.

Lee, J. S., Choi, K. H., Ghim, H. Do, Kim, S. S., Chun, D. H., Kim, H. Y., & Lyoo, W. S. (2004). Role of molecular weight of atactic poly(vinyl alcohol) (PVA) in the structure and properties of PVA nanofabric prepared by electrospinning. *Journal of Applied Polymer Science*, 93(4), 1638 – 1646.

Lee, K. H., Kim, H. Y., Khil, M. S., Ra, Y. M., & Lee, D. R. (2003). Characterization of nano-structured poly( $\epsilon$ -caprolactone) nonwoven mats via electrospinning. *Polymer*, 44(4), 1287 – 1294.

Levingstone, T. J., Matsiko, A., Dickson, G. R., O'Brien, F. J., & Gleeson, J. P. (2014). A biomimetic multi-layered collagen-based scaffold for osteochondral repair. *Acta Biomaterialia*, 10(5), 1996 – 2004.

Lewis, J. L. (1996). Fracture of Articular Cartilage. *Journal of Biomechanical Engineering*, 118(4), 545 – 556.

Li, J., Illeperuma, W. R. K., Suo, Z., & Vlassak, J. J. (2014). Hybrid Hydrogels with Extremely High Stiffness and Toughness. *ACS Macro Letters*, 3(6), 520 – 523.

Li, J., Suo, Z., & Vlassak, J. J. (2014). Stiff, strong, and tough hydrogels with good chemical stability. *Journal of Materials Chemistry B*, 2(39), 6708 – 6713.

Li, L., Lu, C., Wang, L., Chen, M., White, J., Hao, X., McLean, K. M., Chen, H., & Hughes, T. C. (2018). Gelatin-Based Photocurable Hydrogels for Corneal Wound Repair. *ACS Applied Materials & Interfaces*, 10(16), 13283 – 13292.

Li, W.-J., Danielson, K. G., Alexander, P. G., & Tuan, R. S. (2003). Biological response of chondrocytes cultured in three-dimensional nanofibrous poly( $\epsilon$ -caprolactone) scaffolds. *Journal of Biomedical Materials Research*, 67A(4), 1105 – 1114.

Li, W.-J., Jiang, Y. J., & Tuan, R. S. (2006). Chondrocyte phenotype in engineered fibrous matrix is regulated by fiber size. *Tissue Engineering*, 12(7), 1775 – 1785.

Li, Z., & Zhang, M. (2005). Chitosan-alginate as scaffolding material for cartilage tissue engineering. *Journal of Biomedical Materials Research Part A*, 75A(2), 485 – 493.

Liao, S., Ramakrishna, S., & Ramalingam, M. (2012). Electrospun Nanofiber and Stem Cells in Tissue Enigneering. In: Ramalingam, M., Haidar, Z., Ramakrishna S., Kobayashi, H. & Haikel, Y. (Eds.). *Intergrated Biomaterials in Tissue Engineering*. Salem, MA: Scrivener Publishing. 91 – 118.

Lien, S.-M., Ko, L.-Y., & Huang, T.-J. (2009). Effect of pore size on ECM secretion and cell growth in gelatin scaffold for articular cartilage tissue engineering. *Acta Biomaterialia*, 5(2), 670 – 679.

Liguori, A., Uranga, J., Panzavolta, S., Guerrero, P., de la Caba, K., & Focarete, M. L. (2019). Electrospinning of fish gelatin solution containing citric acid: An environmentally friendly approach to prepare crosslinked gelatin fibers. *Materials*, 12(17), 2808.

Lin, S., Cao, C., Wang, Q., Gonzalez, M., Dolbow, J. E., & Zhao, X. (2014). Design of stiff, tough and stretchy hydrogel composites via nanoscale hybrid crosslinking and macroscale fiber reinforcement. *Soft Matter*, 10(38), 7519 – 7527.

Lim, C. T., Tan, E. P. S., & Ng, S. Y. (2008). Effects of crystalline morphology on the tensile properties of electrospun polymer nanofibers. *Applied Physics Letters*, 92(14), 141908.

Liu, J., Li, L., Suo, H., Yan, M., Yin, J., & Fu, J. (2019). 3D printing of biomimetic multi-layered GelMA/nHA scaffold for osteochondral defect repair. *Materials & Design*, 171, 107708.

Loh, Q. L., & Choong, C. (2013). Three-Dimensional Scaffolds for Tissue Engineering Applications: Role of Porosity and Pore Size. *Tissue Engineering Part B: Reviews*, 19(6), 485 – 502.

Lorenz, H., & Richter, W. (2006). Osteoarthritis: Cellular and molecular changes in degenerating cartilage. *Progress in Histochemistry and Cytochemistry*, 40(3), 135 – 163.

Lv, L.-C., Huang, Q.-Y., Ding, W., Xiao, X.-H., Zhang, H.-Y., & Xiong, L. X. (2019). Fish gelatin: The novel potential applications. *Journal of Functional Foods*, 63, 103581.

Mansfield, J. C., Bell, J. S., & Winlove, C. P. (2015). The micromechanics of the superficial zone of articular cartilage. *Osteoarthritis and Cartilage*, 23(10), 1806 – 1816.

Mansour, J. M. (2003). Biomechanics of cartilage. In: Oatis, C. A. *Kinesiology: The mechanics and pathomechanics of human movement*. Philadelphia, PA: Lippincott Williams & Wilkins. 66 – 79.

Martínez-Mejía, G., Vázquez-Torres, N. A., Castell-Rodríguez, A., del Río, J. M., Corea, M., & Jiménez-Juárez, R. (2019). Synthesis of new chitosan-glutaraldehyde scaffolds for tissue engineering using Schiff reactions. *Colloids and Surfaces A: Physicochemical and Engineering Aspects*, 579, 123658.

Mazoochi, T., Hamadani, M., Ahmadi, M., & Jabbari, V. (2012). Investigation on the morphological characteristics of nanofibrous membrane as electrospun in the different processing parameters. *International Journal of Industrial Chemistry*, 3(1), 1 – 8.

McCullen, S. D., Autefage, H., Callanan, A., Gentleman, E., & Stevens, M. M. (2012). Anisotropic Fibrous Scaffolds for Articular Cartilage Regeneration. *Tissue Engineering Part A*, 18(19-20), 2073 – 2083.

Medeiros, E. S., Mattoso, L. H. C., Offeman, R. D., Wood, D. F., & Orts, W. J. (2008). Effect of relative humidity on the morphology of electrospun polymer fibers. *Canadian Journal of Chemistry*, 86(6), 590 – 599.

Megelski, S., Stephens, J. S., Chase, D. B., & Rabolt, J. F. (2002). Micro- and nanostructured surface morphology on electrospun polymer, *Macromolecules*, 35(22), 8456 – 8466.

Michelini, L., Probo, L., Farè, S., & Contessi Negrini, N. (2020). Characterization of gelatin hydrogels derived from different animal sources. *Materials Letters*, 272, 127865.

Moroni, L., Licht, R., de Boer, J., de Wijn, J. R., & van Blitterswijk, C. A. (2006). Fiber diameter and texture of electrospun PEOT/PBT scaffolds influence human mesenchymal stem cell proliferation and morphology, and the release of incorporated compounds. *Biomaterials*, 27(28), 4911 – 4922.

Mow, V. C., Gu, W. Y., & Chen, F. H. (2005). Structure and function of articular cartilage and meniscus. In: Mow, V. C., & Huiskes, R. (Eds.). *Basic Orthopaedic Biomechanics & Mechanobiology*. Lippincott Williams & Wilkins. 181 – 258.

Mow, V. C., Ratcliffe, A., & Poole, A. R. (1992). Cartilage and diarthrodial joints as paradigms for hierarchical materials and structures. *Biomaterials*, 13(2), 67 – 97.

Muller, P., Lemmen, C., Gay, S., von Der Mark, K., & Kiihn, K. (1975). Biosynthesis of Collagen by Chondrocytes in vitro. In: Slavkin, H. C. & Greulich, R. C. (Eds). *Extracellular Matrix Influences on Gene Expression*. Academic Press. 293 – 302.

Naficy, S., Brown, H. R., Razal, J. M., Spinks, G. M., & Whitten, P. G. (2011). Progress toward robust polymer hydrogels. *Australian Journal of Chemistry*, 64(8), 1007 – 1025.

Nataraj, D., Reddy, R., & Reddy, N. (2020). Crosslinking electrospun poly (vinyl) alcohol fibers with citric acid to impart aqueous stability for medical applications. *European Polymer Journal*, 124, 109484.

Nezarati, R. M., Eifert, M. B., & Cosgriff-Hernandez, E. (2013). Effects of humidity and solution viscosity on electrospun fiber morphology. *Tissue Engineering: Part C*, 19(10), 1 – 10.

Nguyen, L. H., Kudva, A. K., Saxena, N. S., & Roy, K. (2011). Engineering articular cartilage with spatially-varying matrix composition and mechanical properties from a single stem cell population using a multi-layered hydrogel. *Biomaterials*, 32(29), 6946 – 6952.

Noriega, S. E., Hasanova, G. I., Schneider, M. J., Larsen, G. F., & Subramanian, A. (2012). Effect of fiber diameter on the spreading, proliferation and differentiation of chondrocytes on electrospun chitosan matrices. *Cells Tissues Organs*, 195(3), 207 – 221.

Nuge, T., Tshai, K. Y., Lim, S. S., Nordin, N., & Hoque, M. E. (2020). Characterization and optimization of the mechanical properties of electrospun gelatin nanofibrous scaffolds. *World Journal of Engineering*, 17(1), 12 – 20.

O'brien, F. J. (2011). Biomaterials & scaffolds for tissue engineering. *Materials today*, 14(3), 88 – 95.

Oei, E. H. G., van Tiel, J., Robinson, W. H., & Gold, G. E. (2014). Quantitative Radiologic Imaging Techniques for Articular Cartilage Composition: Toward Early Diagnosis and Development of Disease-Modifying Therapeutics for Osteoarthritis. *Arthritis Care & Research*, 66(8), 1129 – 1141.

Oh, S. H., Park, I. K., Kim, J. M., & Lee, J. H. (2007). In vitro and in vivo characteristics of PCL scaffolds with pore size gradient fabricated by a centrifugation method. *Biomaterials*, 28(9), 1664 – 1671.

Oinas, J., Ronkainen, A. P., Rieppo, L., Finnilä, M. A. J., Iivarinen, J. T., van Weeren, P. R., Helminen, H. J., Brama, P. A. J., Korhonen, R. K., & Saarakkala, S. (2018). Composition, structure and tensile biomechanical properties of equine articular cartilage during growth and maturation. *Scientific Reports*, 8(1), 1 - 12.



Okutan, N., Terzi, P., & Altay, F. (2014). Affecting parameters on electrospinning process and characterization of electrospun gelatin nanofibers, *Food Hydrocolloids*, 39, 19 – 26.

Padrão, J., Silva, J. P., Rodrigues, L. R., Dourado, F., Lanceros-Méndez, S., & Sencadas, V. (2014). Modifying Fish Gelatin Electrospun Membranes for Biomedical Applications: Cross-Linking and Swelling Behavior. *Soft Materials*, 12(3), 247 – 252.

Park, H., Guo, X., Temenoff, J. S., Tabata, Y., Caplan, A. I., Kasper, F. K., & Mikos, A. G. (2009). Effect of Swelling Ratio of Injectable Hydrogel Composites on Chondrogenic Differentiation of Encapsulated Rabbit Marrow Mesenchymal Stem Cells In Vitro. *Biomacromolecules*, 10(3), 541 – 546.

Park, J. B., & Lakes, R. S. (2007). *Biomaterials: An Introduction*, 3rd ed. New York: Springer.

Park, S.-N., Park, J., Kim, H. O., Song, M. J., & Suh, H. (2002). Characterization of porous collagen/hyaluronic acid scaffold modified by 1-ethyl-3-(3-dimethylaminopropyl) carbodiimide cross-linking. *Biomaterials*, 23(4), 1205 – 1212.

Patterson, J., Siew, R., Herring, S. W., Lin, A. S., Guldborg, R., & Stayton, P. S. (2010). Hyaluronic acid hydrogels with controlled degradation properties for oriented bone regeneration. *Biomaterials*, 31(26), 6772 – 6781.

Pelipenko, J., Kristl, J., Janković, B., Baumgartner, S., & Kocbek, P. (2013). The impact of relative humidity during electrospinning on the morphology and mechanical properties of nanofibers. *International Journal of Pharmaceutics*, 456(1), 125 – 134.

Pelipenko, J., Kocbek, P., & Kristl, J. (2015). Nanofiber diameter as a critical parameter affecting skin cell response. *European Journal of Pharmaceutical Sciences*, 66, 29 – 35.

Peng, Y. Y., Glattauer, V., & Ramshaw, J. A. M. (2017). Stabilisation of Collagen Sponges by Glutaraldehyde Vapour Crosslinking. *International Journal of Biomaterials*, 2017, 1 – 6.

Peters, A. E., Akhtar, R., Comerford, E. J., & Bates, K. T. (2018). The effect of ageing and osteoarthritis on the mechanical properties of cartilage and bone in the human knee joint. *Scientific Reports*, 8(1), 1 – 13.

Pham, Q. P., Sharma, U., & Mikos, A. G. (2006a). Electrospinning of polymeric nanofibers for tissue engineering applications: a review. *Tissue Engineering*, 12(5), 1197 – 1211.

Pham, Q. P., Sharma, U., & Mikos, A.G. (2006b). Electrospun poly(epsilon-caprolactone) microfiber and multilayer nanofiber/microfiber scaffolds: characterization of scaffolds and measurement of cellular infiltration. *Biomacromolecules*, 7(10), 2796 – 2805.

Pillay, V., Dott, C., Choonara, Y. E., Tyagi, C., Tomar, L., Kumar, P., Toit, L. C., & Ndesendo, V. M. K. (2013). A review of the effect of processing variables on the fabrication of electrospun nanofibers for drug delivery applications, *Journal of Nanomaterials*, 2013, 1 – 22.

Portocarrero, G., Collins, G., & Livingston Arinze T. (2013). Challenges in cartilage tissue engineering. *Journal of Tissue Science & Engineering*, 4(1), e120.

Powell, H. M., & Boyce, S. T. (2008). Fiber density of electrospun gelatin scaffolds regulates morphogenesis of dermal-epidermal skin substitutes. *Journal of Biomedical Materials Research - Part A*, 84(4), 1078 – 1086.

Pu, J., & Komvopoulos, K. (2014). Mechanical properties of electrospun bilayer fibrous membranes as potential scaffolds for tissue engineering. *Acta Biomaterialia*, 10(6), 2718 – 2726.

Pu, J., Yuan, F., Li, S., & Komvopoulos, K. (2015). Electrospun bilayer fibrous scaffolds for enhanced cell infiltration and vascularization in vivo. *Acta Biomaterialia*, *13*, 131–141.

Purslow, P. P. (1983a). Measurement of the fracture toughness of extensible connective tissues. *Journal of Materials Science*, *18*(12), 3591 – 3598.

Purslow, P. P. (1983b). Positional variations in fracture toughness, stiffness and strength of descending thoracic pig aorta. *Journal of Biomechanics*, *16*(11), 947 – 953.

Qian, Y.-F., Zhang, K.-H., Chen, F., Ke, Q.-F., & Mo, X.-M. (2011). Cross-linking of gelatin and chitosan complex nanofibers for tissue-engineering scaffolds. *Journal of Biomaterials Science, Polymer Edition*, *22*(8), 1099 – 1113.

Quinn, T. M., Hunziker, E. B., & Häuselmann, H.-J. (2005). Variation of cell and matrix morphologies in articular cartilage among locations in the adult human knee. *Osteoarthritis and Cartilage*, *13*(8), 672 – 678.

Raja Mohd Hafidz, R. N., Yaakob, C. M., & Noorfaizan, A. (2011). Chemical and functional properties of bovine and porcine skin gelatin. *International Food Research Journal*, *18*, 813 – 817.

Rambani, R., & Venkatesh, R. (2014). Current concepts in articular cartilage repair. *Journal of Arthroscopy and Joint Surgery*, *1*(2), 59 – 65.

Repanas, A., Andriopoulou, S., & Glasmacher, B. (2016). The significance of electrospinning as a method to create fibrous scaffolds for biomedical engineering and drug delivery applications. *Journal of Drug Delivery Science and Technology*, *31*, 137–146.

Responde, D. J., Natoli, R. M., and Athanasiou, K. A. (2007). Collagens of articular cartilage: structure, function, and importance in tissue engineering. *Critical Reviews in Biomedical Engineering*, *35*(5), 363 – 411.

Rivlin, R. S., & Thomas, A. G. (1953). Rupture of rubber. I. Characteristic energy for tearing. *Journal of Polymer Science*, 10(3), 291 – 318.

Rnjak-Kovacina, J., & Weiss, A. S. (2011). Increasing the Pore Size of Electrospun Scaffolds. *Tissue Engineering Part B: Reviews*, 17(5), 365 – 372.

Rogina, A. (2014). Electrospinning process: Versatile preparation method for biodegradable and natural polymers and biocomposite systems applied in tissue engineering and drug delivery. *Applied Surface Science*, 296, 221 – 230.

Rönn, K., Reischl, N., Gautier, E., & Jacobi, M. (2011). Current Surgical Treatment of Knee Osteoarthritis. *Arthritis*, 2011, 1 – 9.

Roseti, L., Desando, G., Cavallo, C., Petretta, M., & Grigolo, B. (2019). Articular Cartilage Regeneration in Osteoarthritis. *Cells*, 8(11), 1305.

Roth, V., & Mow, V. C. (1980). The intrinsic tensile behavior of the matrix of bovine articular cartilage and its variation with age. *The Journal of Bone & Joint Surgery*, 62(7), 1102 – 1117.

Sachlos, E., & Czernuszka, J. T. (2003). Making tissue engineering scaffolds work: Review on the application of solid freeform fabrication technology to the production of tissue engineering scaffolds. *European cells and Materials*, 5, 29 – 40.

Salles, T. H. C., Lombello, C. B., & Avila, M. A. (2015). Electrospinning of Gelatin/Poly(Vinyl Pyrrolidone ) blends from water/acetic acid solutions, *Materials Research*, 18(3), 509 – 518.

Sasazaki, Y., Shore, R., & Seedhom, B. B. (2006). Deformation and failure of cartilage in the tensile mode. *Journal of Anatomy*, 208(6), 681 – 694.

Scaffaro, R., Lopresti, F., Botta, L., Rigogliuso, S., & Gherzi, G. (2016). Preparation of three-layered porous PLA/PEG scaffold: relationship between morphology,

mechanical behavior and cell permeability. *Journal of the Mechanical Behavior of Biomedical Materials*, 54, 8 – 20.

Schnabel, M., Marlovits, S., Eckhoff, G., Fichtel, I., Gotzen, L., Vécsei, V., & Schlegel, J. (2002). Dedifferentiation-associated changes in morphology and gene expression in primary human articular chondrocytes in cell culture. *Osteoarthritis and Cartilage*, 10(1), 62 – 70.

Schneider, C. A., Rasband, W. S., & Eliceiri, K. W. (2012). NIH Image to ImageJ: 25 years of image analysis. *Nature methods*, 9(7): 671 – 675.

Shah, R. F., Martinez, A. M., Pedroia, V., Majumdar, S., Vail, T. P., & Bini, S. A. (2019). Variation in the Thickness of Knee Cartilage. The Use of a Novel Machine Learning Algorithm for Cartilage Segmentation of Magnetic Resonance Images. *The Journal of Arthroplasty*, 34(10), 2210 – 2215.

Shankar, K. G., Gostynska, N., Montesi, M., Panseri, S., Sprio, S., Kon, E., Marcacci, M., Tampieri, A., & Sandri, M. (2017). Investigation of different cross-linking approaches on 3D gelatin scaffolds for tissue engineering application: A comparative analysis. *International Journal of Biological Macromolecules*, 95, 1199 – 1209.

Shapiro, J. M., & Oyen, M. L. (2013). Hydrogel composite materials for tissue engineering scaffolds. *Jom*, 65(4), 505 – 516.

Shepherd, D. E., & Seedhom, B. B. (1999). Thickness of human articular cartilage in joints of the lower limb. *Annals of the Rheumatic Diseases*, 58(1), 27 – 34.

Sill, T. J., & von Recum, H. A. (2008). Electrospinning: Applications in drug delivery and tissue engineering. *Biomaterials*, 29(13), 1989 – 2006.

Simpson, D. G., Terracio, L., Terracio, M., Price, R. L., Turner, D. C., & Borg, T. K. (1994). Modulation of cardiac myocyte phenotype in vitro by the composition and orientation of the extracellular matrix. *Journal of cellular physiology*, 161(1), 89 – 105.

Sisson, K., Zhang, C., Farach-Carson, M. C., Chase, D. B., & Rabolt, J. F. (2009). Evaluation of cross-linking methods for electrospun gelatin on cell growth and viability. *Biomacromolecules*, *10*(7), 1675 – 1680.

Sisson, K., Zhang, C., Farach-Carson, M. C., Chase, D. B., & Rabolt, J. F. (2010). Fiber diameters control osteoblastic cell migration and differentiation in electrospun gelatin. *Journal of Biomedical Materials Research - Part A*, *94*(4), 1312 – 1320.

Skotak, M., Noriega, S., Larsen, G., & Subramanian, A. (2010). Electrospun cross-linked gelatin fibers with controlled diameter: The effect of matrix stiffness on proliferative and biosynthetic activity of chondrocytes cultured in vitro. *Journal of Biomedical Materials Research Part A*, *95A*(3), 828 – 836.

Sobral, J. M., Caridade, S. G., Sousa, R. A., Mano, J. F., & Reis, R. L. (2011). Three-dimensional plotted scaffolds with controlled pore size gradients: Effect of scaffold geometry on mechanical performance and cell seeding efficiency. *Acta Biomaterialia*, *7*(3), 1009 – 1018.

Soliman, S., Sant, S., Nichol, J. W., Khabiry, M., Traversa, E., & Khademhosseini, A. (2011). Controlling the porosity of fibrous scaffolds by modulating the fiber diameter and packing density. *Journal of Biomedical Materials Research Part A*, *96A*(3), 566 – 574.

Song, J-H., Kim, H-E., & Kim, H-W. (2008). Production of electrospun gelatin nanofiber by water-based co-solvent approach. *Journal of Materials Science: Materials in Medicine*, *19*(1), 95 – 102.

Songchotikunpan, P., Tattiyakul, J., & Supaphol, P. (2008). Extraction and electrospinning of gelatin from fish skin. *International Journal of Biological Macromolecules*, *42*(3), 247 – 255.

Steele, J. A. M., McCullen, S. D., Callanan, A., Autefage, H., Accardi, M. A., Dini, D., & Stevens, M. M. (2014). Combinatorial scaffold morphologies for zonal articular cartilage engineering. *Acta Biomaterialia*, *10*(5), 2065 – 2075.

Stockwell, R. A. (1967). The cell density of human articular and costal cartilage. *Journal of Anatomy*, 101(4), 753 – 763.

Stockwell, R.A. (1971). The interrelationship of cell density and cartilage thickness in mammalian articular cartilage. *Journal of anatomy*, 109, 411 – 421.

Stok, K., & Oloyede, A. (2003). A qualitative analysis of crack propagation in articular cartilage at varying rates of tensile loading. *Connective Tissue Research*, 44(2), 109 – 120.

Stok, K., & Oloyede, A. (2007). Conceptual fracture parameters for articular cartilage. *Clinical Biomechanics*, 22(6), 725 – 735.

Strange, D. G. T., Tonsomboon, K., & Oyen, M. L. (2014). Mechanical behaviour of electrospun fibre-reinforced hydrogels. *Journal of Materials Science: Materials in Medicine*, 25(3), 681 – 690.

Suekama, T. C., Hu, J., Kurokawa, T., Gong, J. P., & Gehrke, S. H. (2013). Double-Network Strategy Improves Fracture Properties of Chondroitin Sulfate Networks. *ACS Macro Letters*, 2(2), 137 – 140.

Suesca, E., Dias, A. M. A., Braga, M. E. M., de Sousa, H. C., & Fontanilla, M. R. (2017). Multifactor analysis on the effect of collagen concentration, cross-linking and fiber/pore orientation on chemical, microstructural, mechanical and biological properties of collagen type I scaffolds. *Materials Science and Engineering: C*, 77, 333–341.

Sun, B., Long, Y. Z., Zhang, H. D., Li, M. M., Duvail, J. L., Jiang, X. Y., & Yin, H. L. (2014). Advances in three-dimensional nanofibrous macrostructures via electrospinning. *Progress in Polymer Science*, 39(5), 862 – 890.

Sun, L., Li, B., Yao, D., Song, W., & Hou, H. (2018). Effects of cross-linking on mechanical, biological properties and biodegradation behavior of Nile tilapia skin

collagen sponge as a biomedical material. *Journal of the mechanical behavior of biomedical materials*, 80, 51 – 58.

Sun, J.-Y., Zhao, X., Illeperuma, W. R. K., Chaudhuri, O., Oh, K. H., Mooney, D. J., Vlassak., & Suo, Z. (2012). Highly stretchable and tough hydrogels. *Nature*, 489(7414), 133 – 136.

Sung, H.-J., Meredith, C., Johnson, C., & Galis, Z. S. (2004). The effect of scaffold degradation rate on three-dimensional cell growth and angiogenesis. *Biomaterials*, 25(26), 5735 – 5742.

Talebian, A., Kordestani, S. S., Rashidi, A., Dadashian, F., & Montazer, M. (2007). The effect of glutaraldehyde on the properties of gelatin films. *Kemija u industriji: Časopis kemičara i kemijskih inženjera Hrvatske*, 56(11), 537 – 541.

Tan, S. H., Inai, R., Kotaki, M., & Ramakrishna, S. (2005). Systematic parameter study for ultra-fine fiber fabrication via electrospinning process. *Polymer*, 46(16), 6128 – 6134.

Temenoff, J. S., & Mikos, A. G. (2000). Review: Tissue engineering for regeneration of articular cartilage. *Biomaterials*, 21(5), 431 – 440.

Tonsomboon, K., & Oyen, M. L. (2013). Composite electrospun gelatin fiber-alginate gel scaffolds for mechanically robust tissue engineered cornea. *Journal of the Mechanical Behavior of Biomedical Materials*, 21, 185 – 194.

Tonsomboon, K., Butcher, A. L., & Oyen, M. L. (2017). Strong and tough nanofibrous hydrogel composites based on biomimetic principles. *Materials Science and Engineering: C*, 72, 220 – 227.

Tonsomboon, K., Koh, C. T., & Oyen, M. L. (2014). Time-dependent fracture toughness of cornea. *Journal of the Mechanical Behavior of Biomedical Materials*, 34, 116 – 123.



Topuz, F., Abdulhamid, M. A., Holtzl, T., & Szekely, G. (2021). Nanofiber engineering of microporous polyimides through electrospinning: Influence of electrospinning parameters and salt addition. *Materials & Design*, *198*, 109280.

Ulubayram, K., Aksu, E., Gurhan, S. I. D., Serbetci, K., & Hasirci, N. (2002). Cytotoxicity evaluation of gelatin sponges prepared with different cross-linking agents. *Journal of Biomaterials Science, Polymer Edition*, *13*(11), 1203 – 1219.

Uranga, J., Leceta, I., Etxabide, A., Guerrero, P., & de la Caba, K. (2016). Cross-linking of fish gelatins to develop sustainable films with enhanced properties. *European Polymer Journal*, *78*, 82 – 90.

Uyar, T., & Besenbacher, F. (2008). Electrospinning of uniform polystyrene fibers: The effect of solvent conductivity. *Polymer*, *49*(24), 5336 – 5343.

Van Der Schueren, L., De Schoenmaker, B., Kalaoglu, Ö. I., & De Clerck, K. (2011). An alternative solvent system for the steady state electrospinning of polycaprolactone. *European Polymer Journal*, *47*(6), 1256 – 1263.

Vardiani, M., Gholipourmalekabadi, M., Ghaffari Novin, M., Koruji, M., Ghasemi Hamidabadi, H., Salimi, M., & Nazarian, H. (2019). Three-dimensional electrospun gelatin scaffold coseeded with embryonic stem cells and sertoli cells: A promising substrate for in vitro coculture system. *Journal of Cellular Biochemistry*, *120*(8), 12508 – 12518.

Verteramo, A., & Seedhom, B. B. (2004). Zonal and directional variations in tensile properties of bovine articular cartilage with special reference to strain rate variation. *Biorheology*, *41*(3-4), 203 – 213.

Wang, Z., & Liang, L. (2019). Research on quantitative measurement method of articular cartilage thickness change based on MR image. *Journal of Infection and Public Health*, *13*(12), 1993 – 1996.

Wang, Z., & Peng, J. (2014). Articular Cartilage Tissue Engineering: Development and Future: A Review. *Journal of Musculoskeletal Pain*, 22(1), 68 – 77.

Wegst, U. G. K., & Ashby, M. F. (2004). The mechanical efficiency of natural materials. *Philosophical Magazine*, 21(21), 2167 – 2181.

Wei, W., Ma, Y., Yao, X., Zhou, W., Wang, X., Li, C., Lin, J., He, Q., Leptihn, S., & Ouyang, H. (2021). Advanced hydrogels for the repair of cartilage defects and regeneration. *Bioactive Materials*, 6(4), 998 – 1011.

Weiss, C., Rosenberg, L., & Helfet, A. J. (1968). An Ultrastructural Study of Normal Young Adult Human Articular Cartilage. *The Journal of Bone & Joint Surgery*, 50(4), 663 – 674.

Wilder, F. V., Hall, B. J., Barrett, J. P., & Lemrow, N. B. (2002). History of acute knee injury and osteoarthritis of the knee: a prospective epidemiological assessment. *Osteoarthritis and Cartilage*, 10(8), 611 – 616.

Wilson, W., van Donkelaar, C. C., van Rietbergen, R., & Huiskes, R. (2005). The role of computational models in the search for the mechanical behavior and damage mechanisms of articular cartilage. *Medical Engineering & Physics*, 27(10), 810 – 826.

Wong, M., Wuethrich, P., Egli, P. & Hunziker, E. (1996). Zone-specific cell biosynthetic activity in mature bovine articular cartilage: a new method using confocal microscopic stereology and quantitative autoradiography. *Journal of Orthopaedic Research*, 14(3), 424 – 432.

Wong, S.-C., Baji, A., & Leng, S. (2008). Effect of fiber diameter on tensile properties of electrospun poly( $\epsilon$ -caprolactone). *Polymer*, 49(21), 4713 – 4722.

Woo, K. M., Chen, V. J., & Ma, P. X. (2003). Nano-fibrous scaffolding architecture selectively enhances protein adsorption contributing to cell attachment. *Journal of Biomedical Materials Research Part A*, 67(2), 531 – 537.

Woo, K. M., Jun, J. H., Chen, V. J., Seo, J., Baek, J. H., Ryoo, H. M., Kim G. S., Somerman, M. J., & Ma, P. X. (2007). Nano-fibrous scaffolding promotes osteoblast differentiation and biomineralization. *Biomaterials*, 28(2), 335 – 343.

Woodfield, T. B. F., Blitterswijk, C. A. Van, Wijn, J. De, Sims, T. J., Hollander, A. P., & Riesle, J. (2005). Polymer Scaffolds Fabricated with Pore-Size Gradients as a Model for Studying the Zonal Organization within Tissue-Engineered Cartilage Constructs. *Tissue Engineering*, 11(9–10), 1297 – 1311.

Wu, H., Wan, Y., Cao, X., Dalai, S., Wang, S., & Zhang, S. (2008). Fabrication of chitosan-g-polycaprolactone copolymer scaffolds with gradient porous microstructures. *Materials Letters*, 62(17-18), 2733 – 2736.

Wu, S.-C., Chang, W.-H., Dong, G.-C., Chen, K.-Y., Chen, Y.-S., & Yao, C.-H. (2011). Cell adhesion and proliferation enhancement by gelatin nanofiber scaffolds. *Journal of Bioactive and Compatible Polymers*, 26(6), 565 – 577.

Xie, J., Shen, H., Yuan, G., Lin, K., & Su, J. (2021). The effects of alignment and diameter of electrospun fibers on the cellular behaviors and osteogenesis of BMSCs. *Materials Science and Engineering: C*, 120, 111787.

Yeh, M. K., Liang, Y. M., Cheng, K. M., Dai, N. T., Liu, C. C. & Young, J. J. (2011). A novel cell support membrane for skin tissue engineering: Gelatin film cross-linked with 2-chloro-1-methylpyridinium iodide. *Polymer*, 52(4), 996 – 1003.

Yin, D., Wu, Hua., Liu, C., Zhang, J., Zhou, T., Wu, J., & Wan, Y. (2014). Fabrication of composition-graded collagen/chitosan-poly lactide scaffolds with gradient architecture and properties. *Reactive & Functional Polymers*, 83, 98 – 106.

Yodmuang, S., McNamara, S. L., Nover, A. B., Mandal, B. B., Agarwal, M., Kelly, T.-A. N., Chao, P. G., Hung, C., Kaplan, D. L., & Vunjak-Novakovic, G. (2015). Silk microfiber-reinforced silk hydrogel composites for functional cartilage tissue repair. *Acta Biomaterialia*, 11, 27 – 36.

Zhang, L., Hu, J., & Athanasiou, K. A. (2009). The role of tissue engineering in articular cartilage repair and regeneration. *Critical Reviews™ in Biomedical Engineering*, 37(1-2), 1 – 57.

Zhang, Q., Lu, H., Kawazoe, N., & Chen, G. (2013). Preparation of collagen porous scaffolds with a gradient pore size structure using ice particulates. *Materials Letters*, 107, 280 – 283.

Zhang, S., Shim, W. S., & Kim, J. (2009). Design of ultra-fine nonwovens via electrospinning of Nylon 6: Spinning parameters and filtration efficiency. *Materials & Design*, 30(9), 3659 – 3666.

Zhang, Y., Ouyang, H., Chwee, T. L., Ramakrishna, S., & Huang, Z. M. (2005). Electrospinning of gelatin fibers and gelatin/PCL composite fibrous scaffolds. *Journal of Biomedical Materials Research - Part B Applied Biomaterials*, 72(1), 156 – 165.

Zhang, Y. Z., Venugopal, J., Huang, Z.-M., Lim, C. T., & Ramakrishna, S. (2006). Crosslinking of the electrospun gelatin nanofibers. *Polymer*, 47(8), 2911 – 2917.

Zhao, S., Wu, X., Wang, L., & Huang, Y. (2004). Electrospinning of ethyl-cyanoethyl cellulose/tetrahydrofuran solutions. *Journal of Applied Polymer Science*, 91(1), 242 – 246.

Zhao, W., Jin, X., Cong, Y., Liu, Y., & Fu, J. (2013). Degradable natural polymer hydrogels for articular cartilage tissue engineering. *Journal of Chemical Technology and Biotechnology*, 88(3), 327 – 339.

Zhao, X. (2014). Multi-scale multi-mechanism design of tough hydrogels: building dissipation into stretchy networks. *Soft Matter*, 10(5), 672 – 687.

Zhu, B., Li, W., Chi, N., Lewis, R. V., Osamor, J., & Wang, R. (2017). Optimization of Glutaraldehyde Vapor Treatment for Electrospun Collagen/Silk Tissue Engineering Scaffolds. *ACS Omega*, 2(6), 2439 – 2450.

Zhu, D., Tong, X., Trinh, P., & Yang, F. (2018). Mimicking Cartilage Tissue Zonal Organization by Engineering Tissue-Scale Gradient Hydrogels as 3D Cell Niche. *Tissue Engineering Part A*, 24(1–2), 1 – 10.

Zhu, Y., Wan, Y., Zhang, J., Yin, D., & Cheng, W. (2014). Manufacture of layered collagen/chitosan-polycaprolactone scaffolds with biomimetic microarchitecture. *Colloids and Surfaces B: Biointerfaces*, 113, 352 – 360.

Zong, X., Kim, K., Fang, D., Ran, S., Hsiao, B. S. & Chu, B. (2002). Structure and process relationship of electrospun bioabsorbable nanofiber membranes. *Polymer*, 43(16), 4403 – 4412.

Zuo, W., Zhu, M., Yang, W., Yu, H., Chen, Y., & Zhang, Y. (2005). Experimental study on relationship between jet instability and formation of beaded fibers during electrospinning. *Polymer Engineering & Science*, 45(5), 704 – 709.



PTTA UTHM  
PERPUSTAKAAN TUNKU TUN AMINAH